applied sciences

MDPI

Article

Advanced Diagnostics of Aircraft Structures Using Automated Non-Invasive Imaging Techniques: A Comprehensive Review

Kostas Bardis [1,*], Nicolas P. Avdelidis [2,3], Clemente Ibarra-Castanedo [2], Xavier P. V. Maldague [2] and Henrique Fernandes [1,4]

[1] Integrated Vehicle Health Management Centre, Faculty of Engineering and Applied Sciences, Cranfield University, Bedford MK43 0AL, UK; h.fernandes@cranfield.ac.uk
[2] Computer Vision & Systems Laboratory, Department of Electrical & Computer Engineering, Laval University, Quebec City, QC G1V 0A6, Canada; n.p.avdelidis@soton.ac.uk (N.P.A.); clemente.ibarra-castanedo@gel.ulaval.ca (C.I.-C.); xavier.maldague@gel.ulaval.ca (X.P.V.M.)
[3] Department of Aeronautics & Astronautics, School of Engineering, Boldrewood Innovation Campus, University of Southampton, Southampton SO16 7QF, UK
[4] Faculty of Computing, Federal University of Uberlandia, Uberlandia 38408-100, Brazil
* Correspondence: kostas.bardis@cranfield.ac.uk

Abstract: The aviation industry currently faces several challenges in inspecting and diagnosing aircraft structures. Current aircraft inspection methods still need to be fully automated, making early detection and precise sizing of defects difficult. Researchers have expressed concerns about current aircraft inspections, citing safety, maintenance costs, and reliability issues. The next generation of aircraft inspection leverages semi-autonomous and fully autonomous systems integrating robotic technologies with advanced Non-Destructive Testing (NDT) methods. Active Thermography (AT) is an example of an NDT method widely used for non-invasive aircraft inspection to detect surface and near-surface defects, such as delamination, debonding, corrosion, impact damage, and cracks. It is suitable for both metallic and non-metallic materials and does not require a coupling agent or direct contact with the test piece, minimising contamination. Visual inspection using an RGB camera is another well-known non-contact NDT method capable of detecting surface defects. A newer option for NDT in aircraft maintenance is 3D scanning, which uses laser or LiDAR (Light Detection and Ranging) technologies. This method offers several advantages, including non-contact operation, high accuracy, and rapid data collection. It is effective across various materials and shapes, enabling the creation of detailed 3D models. An alternative approach to laser and LiDAR technologies is photogrammetry. Photogrammetry is cost-effective in comparison with laser and LiDAR technologies. It can acquire high-resolution texture and colour information, which is especially important in the field of maintenance inspection. In this proposed approach, an automated vision-based damage evaluation system will be developed capable of detecting and characterising defects in metallic and composite aircraft specimens by analysing 3D data acquired using an RGB camera and a IRT camera through photogrammetry. Such a combined approach is expected to improve defect detection accuracy, reduce aircraft downtime and operational costs, improve reliability and safety and minimise human error.

Keywords: aircraft inspection; defect detection; thermography; visual inspection; defect estimation; photogrammetry; machine-learning; NDT; composites; metallic

Academic Editors: Cesar Levy and Dwayne McDaniel

Received: 20 January 2025
Revised: 13 February 2025
Accepted: 19 March 2025
Published: 25 March 2025

Citation: Bardis, K.; Avdelidis, N.P.; Ibarra-Castanedo, C.; Maldague, X.P.V.; Fernandes, H. Advanced Diagnostics of Aircraft Structures Using Automated Non-Invasive Imaging Techniques: A Comprehensive Review. *Appl. Sci.* **2025**, *15*, 3584. https://doi.org/10.3390/app15073584

1. Introduction

1.1. Structure of the Article

The structure of this article is divided into five chapters. It begins with an introduction to the topic, followed by an overview of common methods and techniques for detecting defects in aircraft structures. The discussion chapter highlights this work's potential contributions to the field and concludes with suggestions for future research on automating aircraft inspections.

Section 1: Introduction—This chapter introduces the challenges of inspecting aircraft structures and explains the importance of automation. It highlights the need to improve safety and efficiency and reduce operating and maintenance costs.
Section 2: Materials and Methods—This chapter analyses the tools, methods, and techniques used, such as thermography, visual, and 3D scanning. It also explores common materials used in the aviation industry, including strengths and limitations, as well as the most common types of defects that appear during inspection. Special attention is given to how artificial intelligence could support these processes to enhance accuracy and reliability.
Section 3: Discussion—This chapter emphasises the intellectual contributions of this research and its potential impact on the aviation industry, the non-destructive testing (NDT) field, and academia.
Section 4: Conclusions—This chapter summarises the findings, highlighting the value of automated inspection. It stresses the importance of integrating AI with advanced tools to enhance outcomes and reduce human errors.
Section 5: Future Directions—This section looks ahead, discussing the scientific aim and the specific objectives this work is willing to address.

1.2. Aircraft Structures and Defect Locations

Aircraft structures are engineered to withstand high aerodynamic loads, temperature variations, and operational stress. The primary structural components, as illustrated in Figure 1, include:

- Fuselage: The main body of the aircraft, housing passengers, crew, and cargo.
- Wings: Provide lift and house fuel tanks and control surfaces.
- Empennage (Tail Section): Ensures stability and control through the horizontal and vertical stabilisers.
- Landing Gear: Supports the aircraft during takeoff, landing, and taxiing.
- Jet Engines: Generate thrust for propulsion.

Over time, these structures are exposed to various mechanical, environmental, and operational stressors, leading to material degradation and defects.

Aircraft materials are primarily metallic (e.g., aluminium, titanium) and composite (e.g., carbon fibre-reinforced polymers, honeycomb structures). As shown in Figure 1, each material type is prone to specific defects based on its composition and operational function.

- Metallic Defects
  - Fuselage: Fatigue cracks, corrosion, pores, and material inclusions.
  - Doors and Structural Joints: Welding issues, foreign inclusions, and adhesive failures.
  - Landing Gear: Overload, wear, and creep due to repeated impact forces.
- Composite Defects
  - Wings: Delamination, fibre/matrix cracking, and impact damage.
  - Tail (Vertical/Horizontal Stabilisers): Honeycomb cell wall damage, core crushing, and skin-to-core debonding.
  - Jet Engines: Thermal stress cracking due to high-temperature exposure.

The early detection of these defects is critical to maintaining aircraft safety, performance, and lifespan.

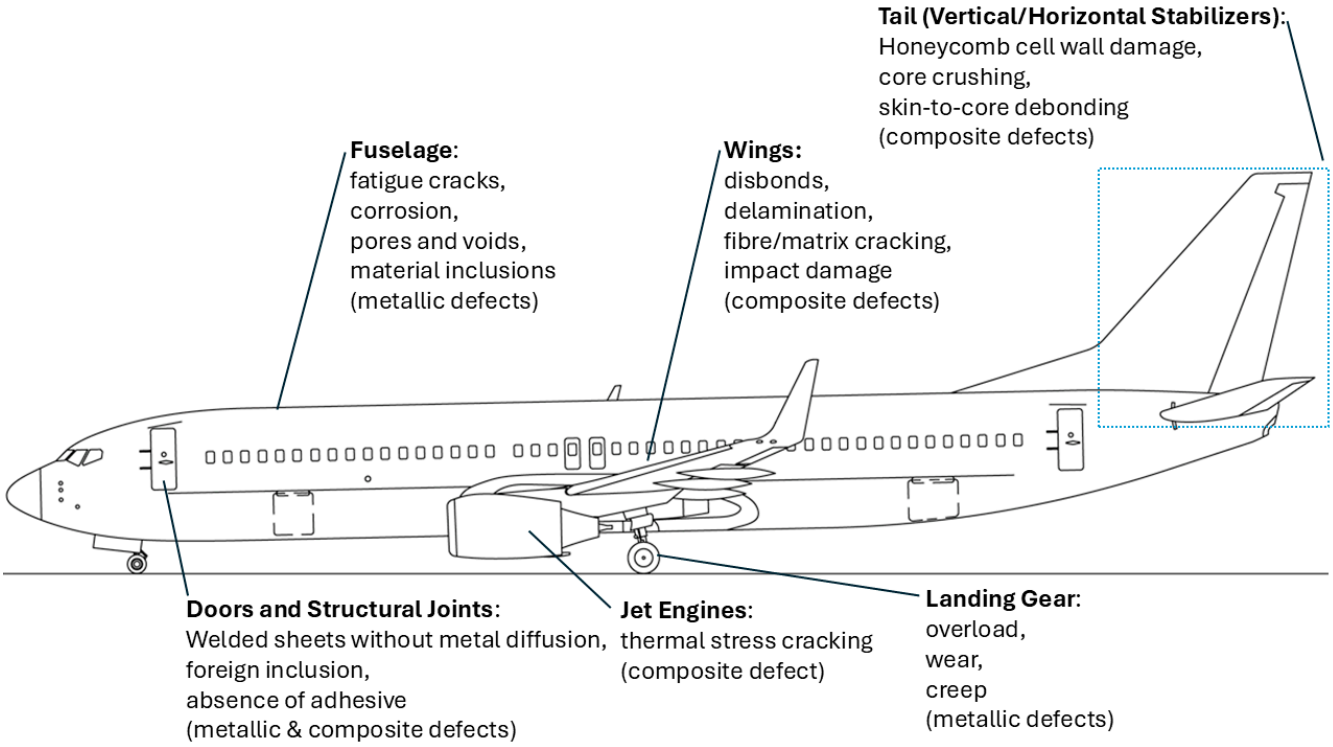

Figure 1. Boeing 737–800 aircraft structure and common defect location [1].

Effective maintenance strategies are essential, given the financial impact of aircraft downtime and structural repairs. Non-Destructive Testing (NDT) and AI-based inspection techniques are increasingly being adopted to reduce operational costs, optimise maintenance schedules, and enhance defect detection accuracy.

1.3. Aircraft Maintenance and Cost Analysis

Aircraft maintenance is crucial in ensuring aircraft reliability, safety, and durability in the aviation industry. In 2022, IATA [2] published a comprehensive report on maintenance cost data. Thirty-one airlines contributed to this report; more specifically, 32,070 aircraft were analysed. The total amount the airlines spent on Maintenance, Repair and Overhaul (MRO) was $76.8 Billion, representing approximately 10.9% of the total airline operational costs ($722 Billion). Another interesting observation from this report was the Global MRO Spend Forecast from 2019 to 2033. Airlines tend to invest more and more money yearly to improve maintenance. Cranfield University [3] estimated the economic impact of an aircraft being out of service due to unscheduled maintenance. The estimated daily losses are approximately £200,000 ($250,560 (calculated using an approximate exchange rate of 1 GBP = 1.253 USD)). This calculation is based on reasonable average estimates, for example, a narrow-body aircraft with 200 passengers, assuming it makes eight daily journeys, and each ticket costs £100 ($125.28). The total losses will be £160,000 ($200,448). Similarly, for a wide-body aircraft with 350 passengers, assuming it makes one journey, and each ticket costs £800 ($1002.24), the total losses will be £280,000 ($350,784). Additionally, Cazzato et al. [4] highlighted the importance of a fully operational aircraft. A 747-cargo liner at Cargolux Airlines S.A. can be in the air for 19 h/day. In other words, an aircraft on the ground produces costs instead of income.

1.4. Human Factor in Aircraft Maintenance

Aircraft maintenance is a complex process, and errors can cause flight delays, cancellations, or, in some cases, incidents and accidents. Over the years, airlines have introduced new technologies to improve maintenance; however, the human factor still plays a crucial role in overall maintenance performance. Some examples of accidents due to human factors are presented below:

- In June 1990, British Airways Flight 5390 had an accident. The left cockpit windscreen was blown out, and the pilot was partially ejected through the open window. After investigation, they found that 84 out of the 90 bolts that fixed the windscreen were smaller in diameter. Due to a staff shortage during maintenance, the shift maintenance manager tried to help by fixing them himself. However, he never checked the maintenance manual, resulting in the incorrect bolt type being used to fix the windscreen [5].
- In 2003, a Raytheon (Beechcraft) 1900D aircraft lost control shortly after takeoff, leading to a crash caused by improper rigging of the elevator control system [6].
- In 2018, Southwest Airlines Flight 1380's engine failed due to a fractured fan blade. Metal fatigue was the leading cause, and debris was inserted into the engine, resulting in a loss of power. The pilots tried an emergency landing; however, one passenger died [7].
- On 15 January 2023, Yeti Airlines Flight 691, was conducting a scheduled domestic flight from Kathmandu to Pokhara International Airport with 68 passengers and 4 crew members. During the final approach to Runway, the aircraft experienced a dual propeller feathering event, leading to a loss of thrust and subsequent aerodynamic stall. The flight crew inadvertently moved the condition levers to the feathered position, preventing thrust recovery. The aircraft crashed near the Seti River gorge, resulting in the fatalities of all 72 individuals on board. The Aircraft Accident Investigation Commission (AAIC) of Nepal identified high workload, human error, inadequate technical training, and non-compliance with SOPs as contributing factors. Nine safety recommendations were issued to improve crew training, approach procedures, and regulatory oversight to prevent similar incidents in the future [8].
- On 6 December 2023, a Qantas Airbus A380 underwent a scheduled three-day maintenance check at Los Angeles International Airport. During a borescope inspection of the left outboard engine, a 1.25 m nylon turning tool was inadvertently left inside the engine. Despite multiple post-maintenance inspections, the tool remained undetected, and the aircraft was released to service on 8 December 2023. Over the next month, the aircraft completed 34 flights totalling 293.74 h before the tool was discovered during a subsequent maintenance check on 1 January 2024. The Australian Transport Safety Bureau (ATSB) investigation revealed failures in tool accountability procedures, including the lack of a formal lost tool search before releasing the aircraft to service. In response, Qantas Engineering revised its tool control policies, emphasising stricter compliance to prevent similar occurrences in the future [9].

The Corporate Aircraft Association (CCA) published a paper [10] in 2016 on Aircraft Maintenance Incident Analysis. The paper highlighted various error types in large aircraft maintenance. Approximately 72% of the reported events involved installation errors and failure to follow specific instructions for task completion. A broader analysis of the associated factors causing installation errors (834) showed that poor inspection was the main factor in many cases, including 223 events in total (please refer to Figure 2).

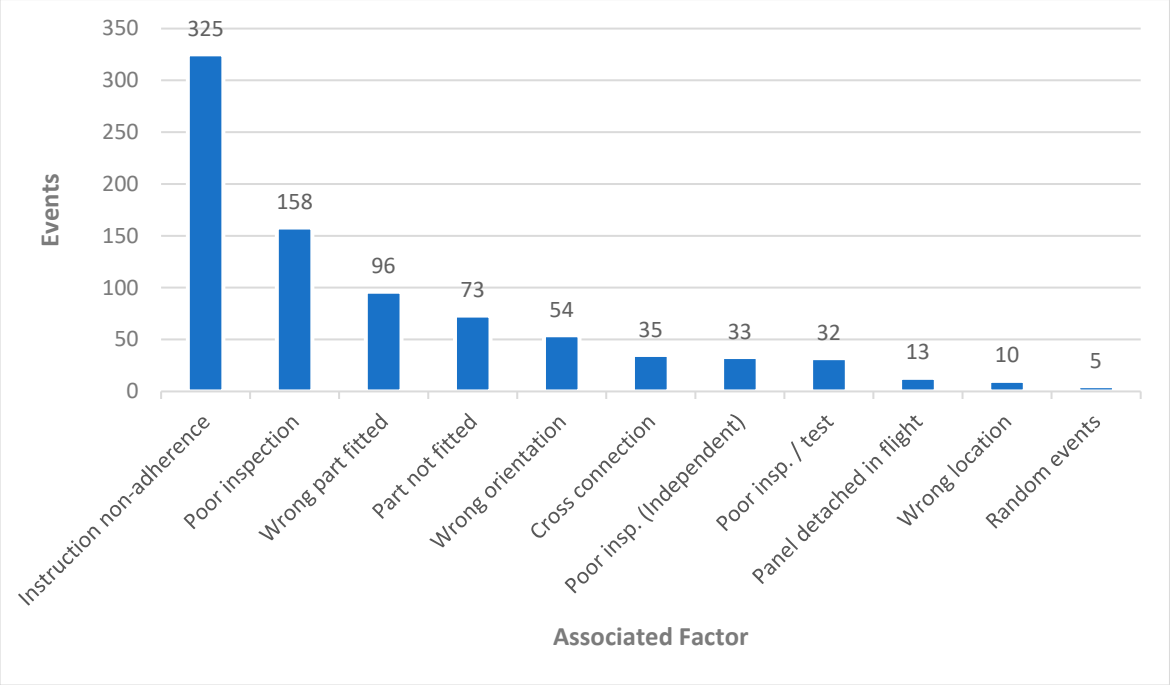

Figure 2. Installation Error and Associated Factors [10].

1.5. Aircraft Maintenance Categories

Olaganathan et al. [5] explained how aircraft maintenance can be categorised into two distinct types: Hangar Maintenance (H.M.) and Line Maintenance (L.M.). H.M. is scheduled for extensive maintenance in a hangar that requires specialised facilities and equipment. H.M. usually takes days or months, and multiple engineers from different areas of expertise work together in some cases simultaneously to perform activities like overhauls, checks, structural repairs, and modifications or upgrades. One of the challenges is the time pressure, as the aircraft must be delivered without any delays to avoid extra losses. Another challenge can be the working conditions, as, in many cases, there are temperature, lighting and noise restrictions. On the other hand, Line Maintenance (L.M.) ensures the aircraft's airworthiness and refers to essential routine maintenance tasks that must be performed daily between flights. These tasks can be performed at the airport gate and mainly involve inspections, minor repairs, and light troubleshooting. If L.M. cannot resolve the issue, H.M. will take over.

In a detailed study of aircraft maintenance personnel's work hours, the Civil Aviation Authority (CAA) highlighted the critical issue of a shortage of licenced engineers and their excessive working hours, which can raise safety concerns. The proposed solution is for the maintenance organisation to implement 24 h shifts, either in three 8 h shifts or two 12 h shifts [11]. As explained earlier, both cases can be stressful and challenging.

The Federal Aviation Administration (FAA) obliges airlines to prepare a mandatory maintenance programme called the Continuous Airworthiness Maintenance Program (CAMP). This process covers day-to-day and detailed inspections called "checks". From lighter to most thorough, there are four levels of checks: A, B, C, and D [12]. Saltoglu et al. [13] provided a summary table (Figure 3) of all four checks, including a brief description, the location, and the frequency/duration for each, arranged in order of increasing complexity.

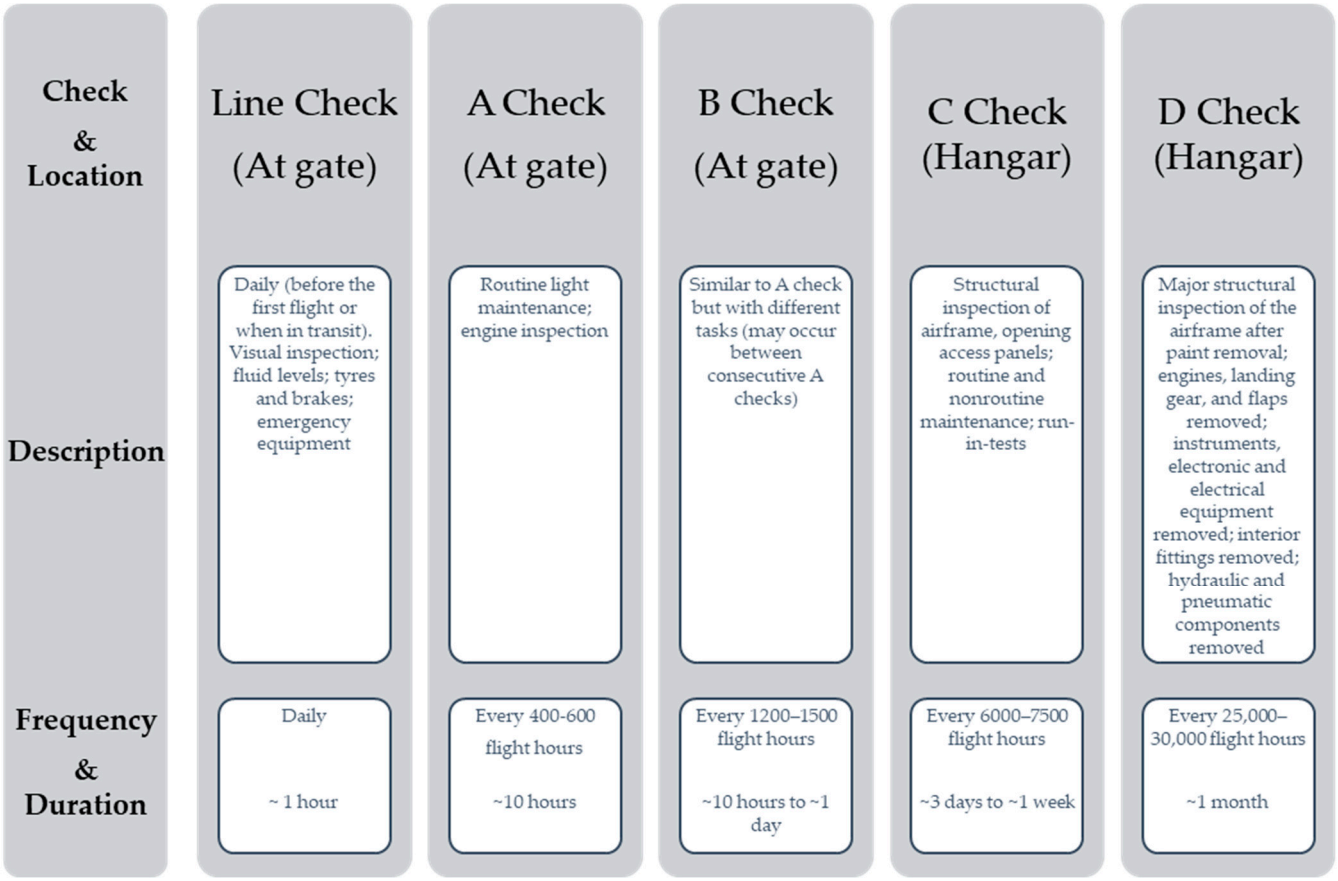

Figure 3. Typical Maintenance Checks [13].

Aircraft maintenance can be further classified into two sub-categories: airframe and engine maintenance. Airframe maintenance focused on electronic systems is referred to as non-structural, while maintenance addressing defects in the structural components, such as fuselage panels, is known as structural airframe maintenance [14].

This research is oriented toward structural airframe maintenance, focusing on Hangar Maintenance checks C and D and improving inspection procedures.

1.6. Manual Inspection

As described earlier, aircraft maintenance, specifically aircraft inspection, is vital, as safety is a top priority in the aviation industry. There are two types of aircraft inspection: visual inspection and non-destructive inspection. Most aviation maintenance inspections—90%—are visual [15]. Papa et al. [16] explained that General Visual Inspection (GVI) is a technical term used in the aerospace sector. This manual process is executed by experienced maintenance engineers using raw human senses like vision, touch, hearing, and smell. Maintenance Steering Group-3 (MSG-3) defines GVI as a "*Visual examination of an interior or exterior area, installation or assembly to detect obvious damage, failure or irregularity, made from within touching distance and under normally available lighting condition such as daylight, hangar lighting, flashlight or drop-light*" [16]. A more detailed analysis of the visual inspection of aircraft was published by the Federal Aviation Administration (FAA) in 1997 [17]. There are four main reasons to perform an aircraft visual inspection:

1. To assess the overall condition of the airframe and components;
2. Defects such as dents, delamination, cracks, and corrosion should be detected early before they reach a critical size;
3. To detect manufacturing defects, in-service defects as well as unplanned defects;

4. Finally, evidence of defects is to be collected to support information about the aircraft's condition.

Depending on the type of check, the certified maintenance engineers walk around the aircraft to perform a casual visual inspection or focus on a specific area or system for an in-depth investigation. They usually use supporting inspection tools and equipment like flashlights, magnifiers, and mirrors. In cases where the inspection area is not reachable, cherry pickers, scissor lifters, ladders, or scaffolding can be used [18]. As Jovančević et al. [19] described, aircraft surface inspection is one of the most crucial maintenance tasks for detecting defects such as cracks, scratches, and dents. However, as his study mentioned, it is very challenging for a human operator to perform without supporting inspection tools. The main reason is the size of the defect, which can be hard or, in some cases, not visible to the naked eye. Low-angle light using a flashlight is a well-known technique quality engineers use to detect defects. Next, the area of interest is demarcated with a marker pen for further examination. The engineer can estimate the defect's size and depth using a dial gauge. The probe moves across the defective area until it contacts the surface. A few disadvantages of this approach include the level of experience of the person performing the measurement and the inability to accurately measure defects larger than the diameter of the dial indicator.

In addition to the previous point, Reyno et al. [20] introduced the ruler and the high-resolution electronic indicator as supporting inspection equipment for dent depth measurement. Multiple manual readings and recordings were required for precision, making it time-consuming, especially with large areas with many dents. Furthermore, data analysis was complex, and further time was required. A circle was drawn to estimate the dent area, with the longest length used to measure the dent's diameter. Measurements varied depending on the inspector's interpretation, and multiple measurements were required for confirmation. In a recent study, Samarathunga et al. [21] presented a new thermography inspection method. Maintenance engineers conducted inspections with manually operated thermography cameras by reaching the designated areas of the aircraft using cranes and jacks. The proposed new methodology was promising; however, the manual process above was time-consuming, raised safety concerns, and depended on the inspector's skills. Cazzato et al. [4] proposed an alternative, safer, cost and time-effective approach using unmanned aerial vehicles (UAVs) based on non-destructive inspection to provide a remote visual assessment.

In summarising the drawbacks of manual visual inspection, the most common issues include the accessibility of the area being inspected, environmental conditions like weather and lighting, inadequate reporting, and human-related factors, all of which can lead to unreliable and inaccurate results. Further analysing the lighting conditions, the Illuminating Engineers Society (IES) [22] suggested direct, focused lighting for inspection checks inside a hangar. More specifically, for a space approximately 10 $\times$ 6 square metres and 4 m high, 800–1100 lux per square metre is required. A high-reflectance wall and floor are essential for the correct and uniform light distribution. As commonly understood, these conditions are only sometimes the case, making the General Visual Inspection even more challenging.

On the other hand, the human factor is also critical, with poor training, failure to follow the proper procedure, and time pressure playing significant roles [23,24]. To incorporate quantitative insights into this literature review, Hobbs et al. [25] reported that nearly 48% of maintenance aircraft inspection failures were attributed to skill-based errors. Contributing factors include insufficient training, a shortage of skilled workers, the absence of appropriate equipment, and unclear maintenance and operating procedures, all of which contribute to human error.

In conclusion, manual visual inspection is questionable, and the introduction of automated visual inspection systems is vital to improving the performance of monitoring an aircraft's structure. In the same direction, Dalton et al. [26] explained the key benefits of an automated aircraft inspection system, highlighting the increase in flight safety, reduction in operating and maintenance costs, and improvement in the aircraft's reliability.

1.7. Automated Inspection and Robotic Systems

In recent years, industrial and academic researchers have contributed to advancing the next generation of aircraft inspection by proposing automated or semi-automated approaches that utilise various technologies such as vortex robots, unmanned aerial vehicles (UAVs), wheeled mobile robots, and robotic arms.

A notable example of a mobile platform is the Air-Cobot wheeled mobile robot, developed by Jovančević et al. [19] in 2017. This system developed a 3D point cloud inspection system capable of detecting and characterising defects on the fuselage of a real Airbus A320 aeroplane. The data were collected with the Artec Eva 3D scanner mounted on the Air-Cobot wheeled mobile robot. Particular attention should be given to the Air-Cobot wheeled mobile robot, which stands out due to its unique combination of Non-Destructive Testing (NDT), Autonomous Navigation, and Human–Robot Interaction (HRI) capabilities. The robot was equipped with a 3D scanner and a PTZ camera for NDT purposes. It could safely navigate autonomously around aircraft, avoiding obstacles. Additionally, the robot was adaptive, meaning it could learn from human interactions and improve its efficiency over time [27–31]. As previously mentioned, the inspection process was fully automated, following a pre-defined trajectory to detect defects such as dents and scratches. Novel techniques were also employed to accurately measure the defects' size, depth and orientation. The system's performance was compared against ground truth measurements using high-precision measuring equipment [19].

Expanding on robotised inspection platforms, Toman et al. [32] developed a prototype vortex adhesion-based robotic system for automated aircraft inspections in real-world environments. Unlike wheeled mobile robots operating on flat surfaces, this solution could move across curved and inclined aircraft structures, such as fuselages and wings. The robot was built for hangar and field conditions, addressing challenges like surface accessibility and environmental variability. Its integration of an eddy current testing (ECT) probe allowed it to detect cracks and corrosion in metallic aircraft components. A key advantage of this system was its modular design. Through laboratory and field testing, the system proved capable of accurately identifying defects, demonstrating the potential of robotic automation in aircraft maintenance.

Another robotized system was introduced by Reyno et al. [20], who proposed a 3D scanning system capable of detecting surface damages during semi-automated aircraft inspections. Specifically, this technology could inspect in-service honeycomb sandwich panels and accurately detect and characterise dents. This promising approach could estimate dent depth with a false error rate within 0.04 ± 0.06 mm. The preferred point cloud acquisition system was the FARO® (Lake Mary, FL, USA) Edge 3D scanning system, consisting of a FARO Laser Line Probe and SmartArm (Toronto, ON, Canada) technology.

Samarathunga et al. [21] adopted a slightly different approach, utilising a "vortex" wall-climbing robot integrated with a heat pump as a stimulation source and an infrared sensor for real-time temperature acquisition. This setup was used to inspect aircraft honeycomb composite structures and detect the presence of water. The inspection was conducted remotely via Bluetooth, and the processed thermal images were validated against those captured by a Fluke thermal camera. The study concluded that the method was sufficiently reliable for detecting water ingress.

Unmanned aerial vehicles (UAVs) are increasingly being recognised for their potential to automate and enhance the process of visual aircraft inspection. In the late 2010s, companies like Blue Bear and Createc, with their RISER project, along with Airbus and its Aircam programme, started focusing on developing automated UAV systems for aircraft inspections [33]. In 2016, Donecle developed its own autonomous UAV [34], offering visual inspection of the exterior of an aircraft. In that direction, Papa et al. [16] conducted research on developing an autonomous UAV equipped with a high-definition camera to inspect aluminium panels, including various defects, such as lightning strikes and hail damage. The UAV was outfitted with multiple distance and trajectory sensors to maintain an optimal distance from the aircraft and to avoid obstacles. Data transmission between the UAV and a PC-based ground station was facilitated through a Wi-Fi link, and a graphical user interface (GUI) was developed in MATLAB/LabVIEW for data processing and presentation. While this was a preliminary design, initial tests demonstrated promising results in defect detection. However, further refinements in fully autonomous trajectory planning are needed. The RC EYE One Xtreme was selected as the micro-UAV for this project, featuring a weight of only 260 g, a payload capacity of 150 g, and a typical flight time of 10 min. The author also highlighted several advantages of using drone-based GVI. First, this approach could be cost-effective and time-efficient compared to conventional visual inspection methods. Significantly reducing the aircraft's maintenance time in the hangar by accelerating visual checks. Additionally, UAVs could safely access hard-to-reach areas, eliminating operator health risks. Defect detection accuracy could be increased by comparing the acquired images with a database containing thousands of previously captured images. Moreover, various data types could be gathered by integrating non-destructive sensors, such as thermal cameras and ultrasound probes.

In 2024, Plastropoulos et al. [35], in collaboration with TUI's airline maintenance team, introduced a drone-based General Visual Inspection (GVI) system. They used a Parrot Anafi drone, which featured a camera mounted on an integrated gimbal, to inspect the surface of a TUI aircraft within a hangar. The data collected was used to train a machine learning model to detect and classify five distinct types of defects automatically. Additionally, they developed a size estimation algorithm to assess the identified defects. The primary objective was to detect dents, and the model demonstrated a precision of 71% with an Area Under the Curve (AUC) of 0.69.

2. Methods and Materials

Aircraft maintenance relies on a combination of Non-Destructive Testing (NDT) techniques, machine learning approaches, and advanced defect characterisation methods to ensure aerospace materials' structural integrity and safety. This section provides a comprehensive overview of the methodologies used for damage detection, defect classification, and size and depth estimation in metallic and composite aircraft structures.

Non-Destructive Testing (NDT) techniques play a crucial role in identifying structural defects without compromising the integrity of the material. Various ultrasonic, radiographic, thermographic, and eddy current-based inspection methods are commonly used to detect subsurface anomalies, corrosion, and material degradation in aerospace components. These techniques allow for accurate and efficient defect characterisation, reducing the need for invasive inspections.

In parallel, machine learning-based approaches have emerged as a powerful tool for automating defect detection and classification. Convolutional Neural Networks (CNNs), Support Vector Machines (SVMs), Mask R-CNN, and ensemble models have significantly improved crack detection, corrosion assessment, and defect segmentation. These AI-

driven techniques leverage large datasets, sensor fusion, and deep learning architectures to enhance aircraft maintenance precision, recall, and defect localisation.

The materials used in aircraft construction, including aluminium alloys, titanium, carbon fibre-reinforced polymers (CFRPs), and hybrid composites, each present unique failure mechanisms such as fatigue cracks, delamination, fibre-matrix separation, and impact damage. Understanding the behaviour of these materials under operational conditions is essential for implementing effective maintenance strategies.

Additionally, size and depth estimation techniques provide critical information for quantifying defect severity. Methods such as structured light 3D scanning, thermographic imaging, and ultrasonic depth profiling enable precise measurement of defect dimensions, allowing engineers to assess structural integrity and predict failure risks.

This section thoroughly explores these methodologies, highlighting their applications, limitations, and advancements in aviation maintenance and health monitoring.

2.1. Non-Destructive Testing (NDT) Techniques

Non-Destructive Testing (NDT) techniques are widely applied across multiple industries beyond aviation, including civil engineering, infrastructure monitoring, and cultural heritage preservation. A notable example of their successful application is demonstrated in the rehabilitation of the Holy Aedicule of the Holy Sepulchre [36]. This study highlighted how a combination of NDT methods—such as Infrared Thermography (IRT), Ground Penetrating Radar (GPR), Ultrasonic Testing (UT), and Digital Microscopy—was employed to assess the preservation state of a historical monument, monitor ongoing rehabilitation works, and evaluate the compatibility of conservation materials and interventions. These techniques were instrumental in detecting defects, monitoring structural integrity, and providing real-time feedback for decision-making throughout the restoration process.

Selecting the most appropriate non-destructive testing technique is crucial. Each technology meets different needs; therefore, the comparison Table 1 below is essential for understanding the applicability of each method, highlighting the advantages, limitations, and types of aircraft defects that can be detected.

Table 1. Comparison of the most common non-destructive testing techniques in aircraft inspection.

Reference	Technology	Test Object	Advantages	Limitations	Suitable Type of Defect to Be Detected
[37–39]	X-ray	Internal Defects	Not limited by material and geometry; most sensitive to volumetric defects	Defect depth limitations; strict installation and safety requirements; high cost	Porosity or Voids Debonding Foreign Bodies
[37–39]	Ultrasonic	Surface and Internal Defects	Sensitive to defects and quick results	Difficult to detect small, thin and complex parts; coupling agent and direct contact with the specimen is required	Porosity or Voids Delamination Debonding Foreign Bodies Cracks
[37–39]	Magnetic Particle	Surface and Near-Surface Defects	Higher sensitivity than ultrasonic or radiographic when testing surface defects	Limited to Ferromagnetic material; difficult to measure the defect depth	Cracks
[37–39]	Penetrant	Surface opening defect	The operation is simple, and the sensitivity is high	Only surface-opening defects can be detected	Surface-opening defects
[37–39]	Eddy Current	Surface and Near-Surface Defects	Highly automated system; time-saving; no couplant required	Limited to conductive material; easy to give a false display	Cracks
[37–39]	Acoustic Emission	Surface and Internal Defects	Effective for active defects	Having issues with the defect size and shape aspects	Porosity or Voids Delamination Debonding Foreign Bodies Cracks

Table 1. *Cont.*

Reference	Technology	Test Object	Advantages	Limitations	Suitable Type of Defect to Be Detected
[37–39]	Infrared Thermography (IRT)	Surface and Near-Surface Defects	Suitable with metallic and non-metallic materials; no contamination or contact of the test piece	The detection depth is not deep enough;	Delamination Debonding Corrosion Impact Damage Cracks
[19,20,40]	3D Scanning—Laser/LiDAR	Surface Defects	High accuracy; non-contact Inspection; quick data acquisition; detailed 3D mapping; suitable for a wide range of materials and geometries	Surface-only detection; reflectivity issues; high equipment cost; environmental sensitivity	Dents Surface wear Surface deformation Corrosion

X-ray [37–39] technology is a widely utilised non-invasive testing method due to its versatility in inspecting objects regardless of their material or geometry, combined with its high sensitivity to detecting volumetric defects. However, it has several limitations, including strict installation and safety requirements, difficulty measuring defect depth, and high installation costs. X-ray effectively detects internal defects such as porosity, voids, debonding, and foreign bodies. Reun et al. [41] recently introduced an X-ray robotic system designed to evaluate the condition of aeronautical parts. The system featured two industrial robots mounted on 5 m tracks, each equipped with X-ray computed tomography (CT) devices. The purpose was to inspect aeronautical composite components for potential defects, such as porosity and inclusions, that might have developed during manufacturing or while in service. This method showed significant promise for using robotised X-ray tomography to detect volumetric defects. However, the accuracy of robot positioning was critical to achieving reliable results. Specifically, the source and detector should be moved simultaneously and precisely on both sides to ensure accurate reconstruction, as any positioning errors could negatively affect the imaging quality.

Ultrasonic [37–39] approaches such as Phased Array Ultrasonic Testing (PAUT), Time-of-Flight Diffraction (TOFD), Pulse-Echo Testing, Guided Wave Testing, and Immersion Testing can be used in aircraft inspection to detect both surface and internal defects. Several advantages of these methods include high sensitivity to defects, quick results, and accurate defect localisation. However, some limitations exist in detecting minor defects and inspecting thin parts with complex geometries. Additionally, a coupling agent is always necessary, and direct contact with the specimen is required. These technologies can detect porosity or voids, delamination, debonding, foreign bodies, and cracks. Zhang et al. [42] made a significant effort to develop an autonomous UAV system integrated with a 5 MHz, dual-crystal ultrasonic transducer to inspect large aluminium plates of varying thicknesses, including those with simulated defects. The ultrasonic transducer was held in a spring-loaded mounting structure to ensure consistent contact force while transmitting ultrasonic acoustic energy through the coupling gel. The UAV ultrasonic system could autonomously inspect and measure thickness at predefined locations on the surface. A comparison between manual ultrasonic inspection and the UAV-based autonomous ultrasonic inspection revealed that the signal amplitude from the autonomous inspection was much weaker. Positioning errors for the UAV were under 87.1 mm, and alignment errors were less than 5 degrees. These issues were caused by factors such as aerodynamic effects near the surface, the ultrasound probe's sensitivity to angular misalignment, and the overloading of the UAV payload.

Magnetic Particle Inspection (MPI) [37–39] is a non-destructive testing (NDT) technique that is particularly effective for detecting surface and near-surface discontinuities, such as cracks, in ferromagnetic materials. This method stands out because of its high

sensitivity to surface imperfections, allowing for more precise detection of surface-breaking defects than other methods like ultrasonic and radiographic testing. MPI is ideal for scenarios where identifying even minor surface defects is critical to maintaining structural integrity and safety. However, the technique is limited to ferromagnetic materials—such as iron, nickel, cobalt, and certain alloys—because only these materials can be effectively magnetised to create the magnetic fields needed for the inspection. As a result, MPI cannot be used on non-ferromagnetic materials like aluminium, copper, or austenitic stainless steel, which restricts its use to specific types of materials. Kikechi et al. [43] conducted a study to examine the performance of four non-destructive testing (NDT) methods in detecting structural defects in an in-service aircraft's landing gear components and engines. The study involved a certified maintenance engineer who used and compared visual testing, ultrasonic inspection, radiography, and magnetic particle inspection to assess each method's accuracy, reliability, and sensitivity. Focusing on the magnetic particle technique, the author outlined the methodology of magnetic particle testing, as illustrated in Figure 4a.

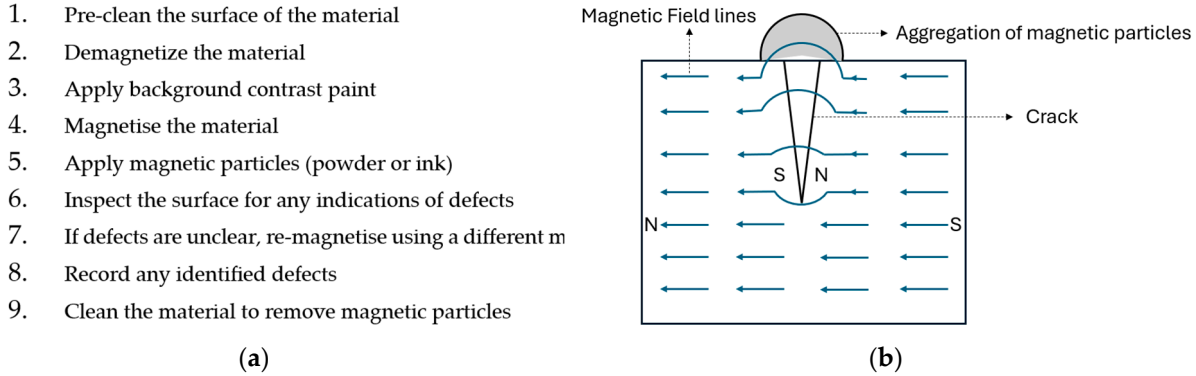

Figure 4. (**a**) Magnetic Particle Inspection testing method [43]; (**b**) Magnetic Particle Inspection working principle of MPI [44].

Suppose there is a defect, such as a crack, a leakage field is created, which attracts magnetic particles and produces a distinct cluster as an indication. Figure 4b is a representative example of a flux leakage from surface and near-surface discontinuities. For near-surface defects, the accumulation of particles is less pronounced, leading to a weaker and less defined indication. The results of this study indicated that the most effective inspection technique was visual inspection using a borescope system, which could detect defects ranging from 1.6 mm to 2.5 mm. In contrast, Magnetic Particle Inspection (MPI) was more sensitive to detecting larger defects, between 4.0 mm and 12.6 mm, located on or just below the surface of ferrous material specimens.

Penetrant [37–39] testing is an easy-to-use, highly sensitive inspection method that is particularly effective at detecting surface-opening defects. While the technique is simple to use and effectively identifies surface anomalies, it is restricted to detecting only those defects that are exposed on the surface, lacking the ability to detect subsurface or near-surface defects. Malandrakis et al. [45] aimed to develop an automated penetrant inspection system using a commercial UAV equipped with a wide-field-of-view camera and an ultraviolet torch to inspect wing panels by flying pre-defined trajectories. Traditional manual penetrant flow inspections are typically time-consuming, taking 1 to 4 h, depending on the object's size. This study introduced an automated, cost-effective, and time-efficient solution for real-time image processing. The proposed non-destructive inspection system detected defects of various sizes, ranging from 2.54 mm to 12.7 mm. The findings indicated that post-processing could enhance reliability, though it would add approximately 2 min to the process. Additionally, further development of the computer vision algorithms was needed to improve the automatic classification and size estimation of defects.

Eddy Current [37–39] is a non-invasive inspection technology based on conductivity, designed to detect surface and near-surface defects. It is highly automated and time-efficient, making it a capable choice for certain applications. A great advantage of this method is that it does not require a couplant between the inspection system and the object. Nevertheless, it is restricted to conductive materials and may sometimes provide inconsistent results, leading to potential confusion. The most common type of defect that Eddy Current can effectively detect is a crack. In 2024, Lysenko et al. [46] evaluated Eddy Current Array (ECA) technology, focusing on aircraft specimens with artificially induced defects of various types, orientations, and sizes to simulate real-world conditions. The study aimed to assess how effective, sensitive, and reliable this technology was in detecting and characterising surface and subsurface defects in aircraft structures. The author also analysed the key factors impacting the performance of this technology, including advantages and limitations. A 360 mm by 120 mm aluminium alloy 31T5 (AD31T5) specimen was fabricated for the experiments, featuring multiple circular defects with varying cluster densities, each with a depth of 4 mm and a diameter of 0.5 mm. This alloy is widely used in the aviation construction industry. A key focus of the study was to assess the ability of ECA technology to detect small defects. For the experiment, the researchers used the Olympus Omniscan MX eddy current flaw detector with a matrix-type eddy current sensor. Due to its flexibility, this sensor could be attached to multiple geometry surfaces, flat or with curves. The results showed that the system could detect clusters of holes; however, it was challenging to detect single holes with such a small diameter of 0.5 mm. Careful calibration of the system, particularly by adjusting sensitivity levels, was crucial to enhance the visibility of defects. This process was challenging, as increasing sensitivity introduced more noise, leading to false positives. In other words, the system mistakenly identified non-defective areas as defective due to the added noise.

Acoustic Emission (AE) [37–39] is a highly effective inspection technology capable of detecting a wide range of defects, including porosity, voids, delamination, debonding, foreign bodies, and cracks. It can identify both surface and internal defects, with particular effectiveness in monitoring active defects. However, AE has limitations, such as difficulty measuring the size and shape of detected defects. Holford et al. [47] analysed the key benefits and limitations of using acoustic emission technology as a structural health monitoring system. Subsequently, they recommended an automated AE monitoring system capable of detecting fatigue fractures in noisy environments and complex structures, such as aircraft's metallic landing gear components. Starting with the advantages, AE technology could be highly capable of continuously inspecting large structures without limitations on defect size. However, some of the mentioned limitations included difficulties in signal characterisation and location accuracy due to complex geometries and background noise. To understand the complexity of this process, the author presented the image below to show the relationship between the source mechanism and digitised signal. The wave propagation path from the source to the sensor could affect the digitised signal. As presented in Figure 5, the type of material and geometry, the coupling method, the sensor itself, and the acquisition hardware could all impact the final result. Changing any of those factors could change the form of the recorded signal compared to the source signal.

In addition, data analysis in AE technology is often complex, requiring considerable operator interpretation and time. A full-scale steel A320 landing gear component was subjected to fatigue loading, with multiple AE sensors carefully placed to monitor it. A fracture initiation was automatically detected after 49,000 fatigue cycles, well before the final failure, as confirmed by a dye penetrant inspection. The fracture's location was determined within 10 mm of its actual position.

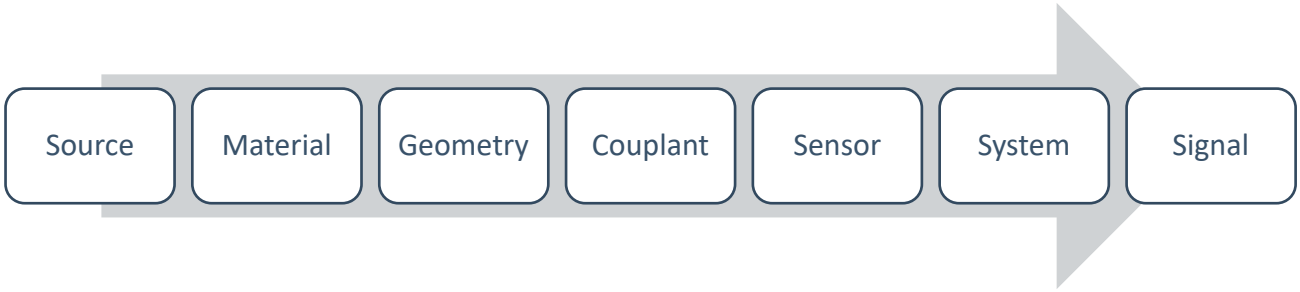

Figure 5. Graphical representation of the AE transfer function [47].

Infrared Thermography (IRT) [37–39] is a widely used, non-invasive aircraft inspection technology capable of detecting surface and near-surface defects, including delamination, debonding, corrosion, impact damage, and cracks. It is suitable for metallic and non-metallic materials and requires neither a coupling agent nor direct contact with the test piece, minimising contamination. However, one of its primary limitations is the relatively shallow detection depth compared to other inspection techniques discussed earlier. As described by Sfarra et al. [48] infrared thermography (IRT) is primarily classified into "passive" and "active" thermography. Passive IRT does not require an external energy source and is typically used when the object being inspected has a significant temperature difference from its surrounding environment. This method is particularly useful for applications involving cyclic loading, as the heat generated during these cycles allows for monitoring temperature variations over time with an infrared (IR) camera. A notable example of passive thermography is the work by Montesano et al. [49], who used this technology to study the fatigue behaviour of carbon fibre-reinforced polymer composites through infrared imaging. On the other hand, Active IRT relies on external excitation sources to create a temperature difference between damaged and undamaged regions of the material being tested. In aerospace applications, the most commonly used active IRT methods based on optical radiation principles include Pulsed Thermography (PT), Lock-In Thermography (LIT), Step-Heating Thermography (SHT), Long-Push Thermography (LPT), Frequency Modulated Thermography (FMT), Laser-spot Thermography (LST), and Laser-line Thermography (LLT) [39]. Table 2 provides a detailed summary of each method, outlining the type of external optical heat source, heating duration, penetration depth, primary applications, and the types of defects in aircraft that each method is best suited to detect.

Alhammad et al. [50] introduced multi-label classification algorithms designed to predict multiple factors simultaneously from thermal images gathered through active thermography, specifically Pulsed Thermography (PT). A total of 24,000 thermal images were captured under various conditions using different geometrically shaped composite material specimens, which were then used to train machine learning models for classification. The measurement system included an X6900 FLIR (Teledyne FLIR LLC, Wilsonville, OR, USA) infrared camera equipped with an InSb-CCD Matrix Sensor, two Fx60 (Balcar, France) photographic flashes that generated a heat flux for a duration of 2 milliseconds, a control unit to synchronise data acquisition with pulse generation and a data processing unit (Figure 6).

The evaluation results showed that the proposed methods performed well in making accurate predictions. The findings suggested that the approaches used, like the RF MLC model (Random Forest multi-label classification) and the use of statistical features in the dataset, were very promising options for classifying a comparative investigation for the non-destructive testing of honeycomb structures by holographic interferometry thermal images of composite materials.

Table 2. Comparison table of most common methods used in optically stimulated active thermography in the aerospace industry [39].

Method	Heat Source	Heating Duration	Depth of Penetration	Primary Application	Suitable Aircraft Defect
PT	High-energy flash/laser	Short, intense pulse	Shallow to medium	Surface and near-surface defects	Surface cracks, delamination, impact damage
LIT	Modulated laser/halogen lamp	Modulated, periodic	Medium	Deeper subsurface defects	Fatigue cracks, corrosion, bonding defects
SHT	Infrared lamps/heaters	Gradual, continuous heating	Medium to deep	Subsurface and deep defects	Delamination, deep cracks, corrosion
LPT	Continuous lamp/laser	Extended duration	Deep	Deeper subsurface defects	Corrosion, internal cracks, delamination
FMT	Frequency-modulated energy source	Variable frequency pulses	Medium to deep	Subsurface defect detection	Delamination, debonding, cracks
LST	Focused laser spot	Focused, short pulse on a spot	Shallow	Localised defect detection	Localised cracks, impact damage
LLT	Laser line	Focused, continuous line heating	Medium	Defect detection along a line	Cracks, corrosion along structural lines

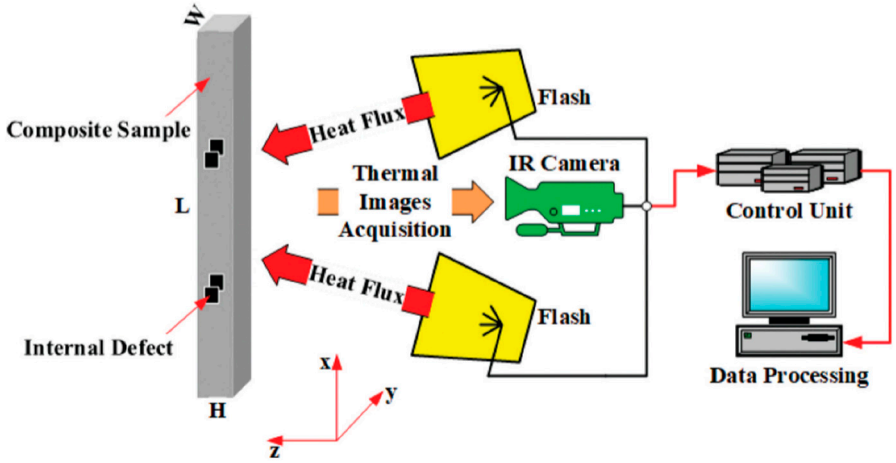

Figure 6. The schematic diagram for the thermography test [50].

A newer option for non-destructive testing (NDT) in aircraft maintenance is 3D scanning [19,20,40], which uses laser or LiDAR (Light Detection and Ranging) technologies. This method effectively detects surface defects like dents, wear, deformation, and corrosion. Its benefits include being non-contact, highly accurate, and fast in collecting data. It also works well with different materials and shapes, producing detailed 3D models. However, it is limited to detecting surface defects, the equipment can be expensive, and environmental factors like reflections can affect the results. Three-dimensional technology has already been applied across many industries, improving medical diagnosis [51,52], aiding in the preservation of historical assets [53], supporting maintenance in manufacturing [54], enriching STEM education [55] and benefiting numerous other fields. Three-dimensional laser scanning involves using a laser beam to precisely capture the shape and geometry of a real-world object in digital form [56]. Three-dimensional laser scanners precisely capture the size and shape of real-world objects, generating point clouds of data to create detailed three-dimensional digital models. This method is especially accurate for inspecting and measuring curved surfaces, providing a more comprehensive description than conventional measurement techniques [57]. Three-dimensional LiDAR (Light Detection and Ranging) scanning uses pulsed laser beams to measure distances by calculating the time it takes for the light to bounce back from an object. This creates a detailed point cloud, producing a three-dimensional digital map of the environment [58]. Table 3 highlights the key distinc-

tions between laser scanning and LiDAR scanning, focusing on aspects such as purpose, method, applicability, range, accuracy, and data output.

Table 3. Critical differences between laser scanning and LiDAR scanning [59,60].

Aspect	Laser Scanning	LiDAR Scanning
Purpose	High-precision scanning of objects or structures to create detailed 3D models	Large-scale mapping and environmental scanning using distance measurement
Method	Uses a laser beam to measure reflected light and capture an object's shape and dimensions	It uses pulsed laser beams to measure the time it takes for light to reflect and return, creating 3D maps
Best For	Capturing small to medium-sized objects in great detail	Mapping large areas and scanning complex environments
Typical Applications	Manufacturing, architecture, reverse engineering, 3D modelling of surfaces	Topography, forestry, urban planning, autonomous vehicles
Range	Short to medium range (up to several metres)	Long range (hundreds of metres to kilometres)
Accuracy	Extremely high, capturing fine surface details	High, but typically less detailed than laser scanning
Data Output	Point clouds representing detailed object surfaces	Point clouds representing wide-area 3D maps

Thulasy et al. [40] used the FARO Focus 3D X130 laser scanner (FARO Technologies, Inc., Lake Mary, FL, USA) in a research project aimed at developing 3D scanning technology capable of inspecting an entire Su-30MKM aircraft (Irkut Corporation, Irkutsk, Russia) and its components. The key innovation of this research was the creation of relevant 3D models to assist the maintenance team in enhancing aircraft maintenance operations and supporting reverse engineering processes. Three-dimensional laser scanning could achieve high acquisition speeds, ranging from hundreds to tens of thousands of data points per second, making it an ideal approach for inspection tasks. As a result, a complete scan could be accomplished in a matter of hours or days, depending on the object's size. The maintenance engineers scanned the aircraft from six angles, merging and aligning the resulting point clouds to create a comprehensive 3D model. The study concluded that 3D scanning could be beneficial for assessing damages with sub-millimetre accuracy. Notably, the Royal Malaysian Air Force used this technology to develop an Illustrated Parts Catalogue (IPC) for the Su-30MKM aircraft and its components.

An alternative approach to 3D scanning, compared to laser or LiDAR technologies, is photogrammetry. This method involves capturing 2D images from multiple angles and using 3D computer vision software to reconstruct a 3D model of the object. Below are the key benefits of using photogrammetry compared to laser and LiDAR scanning:

- Cost-Effectiveness: A good-quality camera and image-processing software are the two essential tools required to scan and reconstruct the 3D model compared to expensive specialised laser and LiDAR equipment [61];
- Detailed Texture Information: A critical advantage of photogrammetry is its ability to acquire high-resolution texture and colour information, which is especially important in the field of maintenance inspection where detailed textures and geometric information are so important [62];
- Versatility and Large-Area Coverage: Photogrammetry can be used for both large-scale and small-scale objects without concerns about geometry, texture, distance from the camera, or the speed of image capture. The use of drones for photogrammetry can be a great combination to capture large areas for mapping efficiently [63].

On the other hand, photogrammetry loses precision compared to laser and LiDAR technologies, particularly with fine geometries [62]. Moreover, photogrammetry relies on

environmental conditions such as weather and lighting, contrasting with LiDAR, which can operate in low light or darkness [63]. Photogrammetry has already been successfully used in fields like forensic science [64], civil infrastructure [65], and archaeology [66]. To the best of my knowledge, no specific study has directly explored the application of photogrammetry for aircraft defect inspection.

A notable example of this technology comes from NASA [67], where photogrammetry was combined with small, unmanned aircraft systems (sUAS) to inspect both the interior and exterior of the AEDC National Full-Scale Aerodynamics Complex (NFAC) wind tunnel facilities at NASA Ames Research Centre. The primary objective of this system was to detect both existing and missing fasteners, as well as to precisely determine their real-world locations in 3D space. This methodology involved object detection algorithms to identify and highlight fasteners and missing fasteners using bounding boxes and photogrammetry to map the detected objects and establish the 3D locations of these defects. Deep learning methods and, more specifically, convolutional neural networks (ResNet18 Mask R-CNN) were the preferred computer vision approaches to detect image defects. A big challenge was the size of the objects to be detected, as most were smaller than 128 × 128 pixels. On the other hand, Pix4D was used to process the set of 2D images to generate the 3D point cloud. In terms of 3D localisation, the researchers used the following algorithm:

1. Creation of a 3D Point Cloud: A 3D point cloud was generated to represent the spatial structure of the environment or objects.
2. Key Point Verification in 2D Images: Each key point in the 2D image was checked to determine if it falls within the bounding box representing part of an object. If it does, this key point was associated with that object.
3. Grouping of Key Points Across Multiple Images: When the same key point was visible in multiple images or on different parts of the object, these key points were grouped together, creating a "set" of similar detections.
4. Estimation of 3D Locations: Once key points were grouped, their 3D spatial positions were analysed to estimate the location of each object.
5. Application of Mean Shift Clustering for Precision: To refine the estimated location of each object, mean shift clustering was applied. This technique identified areas with high concentrations of key points, indicating the most probable 3D location of the object.
6. Confirmation of Object Position through Maxima Identification: Areas where key points densely cluster (known as maxima) provide high confidence that an object is located within that specific 3D space.

The researchers used frame-mAP and video-mAP metrics to evaluate the results quantitatively. The system detected existing fasteners with a frame-mAP of 92.1% and missing fasteners with a frame-mAP of 31%. At the video level, the method achieved an average precision of 86.4% for existing fasteners and 0% for missing fasteners. The low performance in detecting missing fasteners was primarily due to their small size, which the model was unable to detect, as well as the limited and inadequate dataset available for training the model.

Particular attention should be given to the most commonly used open-source photogrammetric software solutions, including COLMAP, OpenMVG + OpenMVS, and AliceVision. While these solutions are generally reliable and robust, they may, in some cases, produce results that lack completeness and accuracy. In this context, Stathopoulou et al. [68] conducted a comprehensive review and evaluation to compare these three open-source image-based 3D reconstruction pipelines, assessing their reliability and performance on large and extensive datasets.

Table 4 compares the capabilities of the three 3D reconstruction pipelines: COLMAP, OpenMVG, and AliceVision. These tools follow similar steps in the 3D reconstruction process; however, each one has unique features.

Table 4. Architecture and key features of open-source image-based 3D reconstruction pipelines analysed in [68].

	COLMAP	**OpenMVG**	**AliceVision**
Key point extraction	SIFT [69]	SIFT [69] AKAZE [70]	SIFT [69] AKAZE [70]
Key point matching	Exhaustive, Sequential, Vocabulary Tree [71] Spatial [72] Transitive [72]	Brute Force, ANN [73] Cascade Hashing [74]	ANN [73] Cascade Hashing [74]
Geometric verification	4 points homography [75] 5 points relative pose [76] 7–8 points F-matrix [75]	4 points homography [75] 5 points relative pose [76] 7–8 points F-matrix [75]	4 points homography [75] 5 points relative pose [76] 7–8 points F-matrix [75] homography growing [77]
Incremental bundle (image resection and triangulation)	P3P [78] + DLT, EPnP [79] + DLT	P3P [78] + DLT, EPnP [79] + DLT	PnP [78] + DLT
Global bundle adjustment	CERES [80]	CERES [80]	CERES [80]
Dense point cloud generation	Patch-based stereo [81]	Patch-based stereo [82]	Semi Global Matching [83]

1. Key Point Extraction: All three tools use the SIFT algorithm to detect key points in images. Additionally, AliceVision supports AKAZE, providing flexibility for different types of image features.
2. Key Point Matching: This step aligns similar points between images. COLMAP offers a variety of methods, including exhaustive, sequential, vocabulary tree, spatial matching, and a transitive option. OpenMVG uses brute force and approximate nearest neighbour (ANN) matching, while AliceVision relies on ANN and cascade hashing for faster matching.
3. Geometric Verification: All tools support verifying geometric relationships using homography estimation (using 4 points), relative pose estimation (using 5 points), and fundamental matrix estimation (using 7–8 points). AliceVision also includes an additional homography growing method for a more robust verification.
4. Incremental Bundle Adjustment: In the image resection and triangulation phase, COLMAP and OpenMVG both use P3P, DLT, and EPNP algorithms. AliceVision simplifies this step with just PnP and DLT, which are standard approaches for pose estimation and triangulation.
5. Global Bundle Adjustment: All three tools use the CERES solver to optimise the 3D model by adjusting camera poses and point positions.
6. Dense Point Cloud Generation: COLMAP and OpenMVG both use a patch-based stereo method to generate a dense point cloud. AliceVision, however, uses semi-global matching, a different approach that balances detail and processing speed.

The study [68] primarily examined image orientation (SfM) and dense reconstruction (MVS) result using indicators like the number of successfully oriented images, reprojection error, and cloud-to-cloud (C2C) distance to ground truth data. COLMAP showed the best overall performance across multiple datasets, especially when using exhaustive matching. It consistently managed to orient a high number of images and kept RMS reprojection errors low, highlighting its reliability in both image orientation and dense reconstruction. OpenMVG, particularly when combined with OpenMVS for dense reconstruction, also performed well, achieving similar reprojection accuracy and completeness, especially on

datasets like 3DOMcity. This makes OpenMVG + OpenMVS a strong option for tasks focused on dense reconstruction. AliceVision showed effective results in certain scenarios but had some difficulty delivering consistent performance across diverse datasets. In some cases, it oriented fewer images and had higher reprojection errors compared to COLMAP and OpenMVG. While AliceVision works well in specific situations, it currently lacks the flexibility and robustness that COLMAP and OpenMVG provide, which makes it less suitable for more complex or large-scale projects.

2.2. Learning-Based Approaches

Machine learning is essential in modernising aircraft maintenance by making defect detection faster and more accurate. By examining patterns in images, these methods improve inspection speed and reliability, helping reduce human mistakes and increase safety. Machine learning techniques have also been successfully applied in various fields beyond aviation, demonstrating their adaptability and effectiveness in complex inspection tasks.

A notable example is their application in cultural heritage preservation, as highlighted in a recent study [84] on the automated detection of rising dampness in historical masonries. This research integrated deep learning with Infrared Thermography (IRT) to identify moisture-related deterioration in historical structures, such as the Holy Aedicule of the Holy Sepulchre and the Msma'a historical building. Using a combination of the PSPNet image segmentation model with a ResNet-50 backbone, the study achieved high accuracy (0.93) and Intersection over Union (IoU) (0.89) despite working with a relatively small dataset. The results underscored the potential of AI-driven models in enhancing the precision of non-destructive testing while ensuring cost-effective and non-intrusive monitoring. The successful implementation of machine learning in this field further reinforces its transformative role in improving inspection processes across different industries, including aviation.

Table 5 provides a snapshot of various machine-learning approaches used in aircraft inspection. Each row presents a specific study and details key components: feature extraction, classifier, ROI selection, data processing, performance metrics, type of defect, environment and libraries, and dataset. The feature extraction section covers techniques like CNNs, which help highlight important image details related to defects. Classifier choices include models like SVMs and neural networks for classifying and detecting faults. ROI selection shows how methods target defect-prone areas to focus computational power where it matters most. Data processing improves image clarity and balances datasets, while performance metrics like accuracy and recall show how effective each approach is. The type of defect points out the specific issues each study aims to detect, from cracks to corrosion. Environment and libraries list the software and tools that make these methods possible, like MATLAB or TensorFlow. Finally, dataset details describe the data used, including image size, resolution, and balance. In the following sections, we will examine how these studies enhance aircraft inspection, discussing strengths, challenges, and their impact on maintenance.

Table 5. Summary table—Architecture and key features of machine learning inspection algorithms in the aviation industry.

Author	Year	Feature Extractor	Classifier	Selection of ROI	Performance Metrics	Type of Defect	Data Processing	Environment/ Libraries	Dataset
Congqing Wang [85]	2016	❖ Angular second moment, Contrast, Correlation Entropy ❖ Echo height Echo time. ❖ Gray level co-occurrence matrix (GLCM)	Multi-class Support Vector Machine (SVM), optimised with a Genetic Algorithm (GA)	N/A	❖ Recognition accuracy of 93.3% ❖ Time Consuming (s) = 61.35342	❖ cracks	❖ Data fusion ❖ GA was employed to optimise the SVM model	❖ MATLAB R2008a	❖ 150 images ○ 30 normal images ○ 60 crack images ○ 30 corrosion images ○ 30 brunt images
Touba Malekzadeh [86]	2017	CNN pre-trained on ImageNet: AlexNet [87] and VGG-F [88]	SVM with a linear kernel	SURF Interest Point Extractor [89]	❖ Accuracy = 0.96 ❖ Sensitivity = 0.96 ❖ Specificity = 0.96 ❖ Processing Time = 15 s	❖ Defect/No Defect	❖ Binary mask ❖ Data-level balancing method ❖ A low-pass Gaussian filter	❖ MAT-LAB/MatConvNet [90]	❖ Unbalance ❖ JPEG format ❖ RGB ❖ 3888 × 5184 resolution
Julien Miranda [91]	2019	ResNet50 (fine-tuned)	Hybrid approach combining CNN with Prototypical Networks for few-shot learning	N/A	❖ Precision = 0.97 ❖ Recall = 0.77 ❖ AP = 0.79	❖ Lightning burns ❖ Paint defects ❖ Rivet ❖ Rivet rash ❖ Screw ❖ Screw rash	❖ Data augmentation and few-shot learning for rare defects	❖ Python, using libraries for CNN and few-shot learning	❖ UAV-acquired high-resolution images ❖ 15; 000 samples ❖ The dataset is highly imbalanced
Julien Miranda [33]	2019	CNN with models like SSD (Single Shot Detector) and YOLO (You Only Look Once)	Generative Adversarial Network (GAN) to create prior patterns for matching detected screws	Manually identified as Zones of Interest (ZOIs) focused on screws	❖ Precision > 95% ❖ Recall > 95%	❖ Missing or loose screws on the aircraft fuselage	❖ Depth maps ❖ GANs	❖ Not specified	❖ Acquired using a UAV with precise laser positioning technology
Soufiane Bouarfa [92]	2020	Mask R-CNN	N/A	N/A	❖ Precision = 69% ❖ Recall = 57%	Dents	❖ Data Augmentation	❖ Annotation = VGG Image Annotator [93] ❖ Python + Python packages: {numpy, Scipy, Pillow, Cython, Matplotlib, Scikit-image, tensorflow >= 1.3.0, keras >= 2.0.8, Opencv-python, H5py, Imgaug, IPython} IDE = MS VS2017	❖ COCO data ❖ The photos were taken from the Abu Dhabi Polytechnic hangar

Table 5. *Cont.*

Author	Year	Feature Extractor	Classifier	Selection of ROI	Performance Metrics	Type of Defect	Data Processing	Environment/ Libraries	Dataset
Ivan Ren [94]	2020	Pre-trained CNNs: VGG, GoogLeNet, and ResNet with 18, 34, and 50 layers	3 CNN base learners (ResNet18, GoogLeNet, and VGG11_bn) Homogeneous (three ResNet18 models), Dimensionally diverse (ResNet18, ResNet34, ResNet50), and Structurally diverse (ResNet18, GoogLeNet, VGG11_bn)	An ROI of 672 × 448 pixels was manually selected and then divided into smaller 224 × 224 images	3x ResNet18 ❖ mean accuracy: 99.8%, ❖ mean precision: 99.61%, ❖ mean F1 score: 99.7%, ❖ mean recall: 100%. ❖ The stacked ensemble models outperformed individual base models in all key metrics, including precision, accuracy, recall, and F1 score.	❖ cracks ❖ corrosion ❖ scratches ❖ gouges	❖ Data augmentation ❖ A cross-entropy loss function ❖ Stochastic gradient descent (SGD) with momentum was used for optimisation, with an early stopping strategy to prevent overfitting.	❖ The models were implemented in PyTorch, with logistic regression trained in scikit-learn.	❖ Collected from borescope inspections of aircraft propeller blades ❖ Balanced dataset of 600 images (300 with defect and 300 defect-free).
Nicolas P. Avdelidis [95]	2022	Pretrained CNN: DenseNet201	Ensemble of CNN models (EfficientNetB1, EfficientNetB5, EfficientNetB4, DenseNet169)	Manual cropping with Python script	❖ DenseNet201 achieved an accuracy of 81.82%. ❖ For defect classification, specific defects were classified with up to 100% accuracy	❖ Missing or Damaged Exterior Paint and Primer ❖ Dents ❖ Reinforcing Patch Repairs ❖ Nicks/ Scratches/Gouges ❖ Blend/Rework Repairs ❖ Lighting Strike Damage ❖ Lighting Strike Fast Repairs	❖ Cropping ❖ Grayscale conversion ❖ Data augmentation ❖ Transfer learning ❖ Early stopping and reduced learning rates were used to optimise the models.	❖ TensorFlow	❖ Custom dataset with 1059 images (576 with defects, 483 without defects). ❖ Captured using a UAV with a Sony RX0 II camera ❖ 4800 × 3200 pixel resolution images in RGB. ❖ Imbalanced dataset
Meng DING [96]	2022	ResNet-50 backbone, pre-trained on ImageNet	Improved Mask Scoring R-CNN framework. A new classifier head with four convolutional layers and a fully connected layer	A Region Proposal Network (RPN) identifies Regions of Interest (ROIs) automatically	❖ Significant improvements over Mask R-CNN and Mask Scoring R-CNN, with a 21% increase in segmentation precision and a 19.59% increase in pixel-level accuracy ❖ Average Precision, Bounding Box of 64.8% ❖ APM (Average Precision, Mask) of 62.7%	❖ Paint detachment ❖ Surface scratches	❖ Convolutional Block Attention Module (CBAM) to enhance significant features ❖ A feature fusion module for multiscale representation. ❖ Data augmentation	❖ Python 3.6.10, ❖ Utilising the Mask Scoring R-CNN ❖ Labelme software	❖ Custom dataset of 276 images of A320 and B737 aircraft skin defects ❖ 960 × 720 resolution ❖ The images capture defects on the fuselage, wings, and tail

Table 5. *Cont.*

Author	Year	Feature Extractor	Classifier	Selection of ROI	Performance Metrics	Type of Defect	Data Processing	Environment/ Libraries	Dataset
Benedict E. Jaeger [97]	2022	CNN architecture: ResNet-18	The ResNet-18 CNN was adapted for binary classification (crack or no crack)	For the SIM, 64 × 64-pixel patches were cropped from specific regions in the larger images	❖ LIM achieved an F2-score of 0.60 on validation ❖ SIM attained 0.85	❖ cracks in turbine blades	❖ Data augmentation ❖ Stratified k-fold cross-validation ❖ Oversampling ❖ Focal loss ❖ Two configurations: a large image model (LIM) and a small image model (SIM)	❖ Fastai ❖ PyTorch	❖ Thermographic images ❖ Class imbalance (crack and crack-free). ❖ LIM used 512 × 640 images (600 crack-free, 52 with cracks), and SIM used 64 × 64 patches derived from these images
Xueyan Oh [98]	2024	A PoseNet, adapted with an Xception backbone Trained on ImageNet	Not available	The model operated on images captured from quadrants defined around the aircraft to localise each scan image	❖ Median localisation error under 0.24 m ❖ Angular error below 2°	Focused on the spatial localisation of visual inspection images on the aircraft's surface	❖ Synthetic images are generated with domain randomisation	❖ TensorFlow	❖ 4000 synthetic images ○ 700 validation and ○ 300 test images.

Wang et al. [85] (2016) proposed a multi-source sensor approach for aircraft skin crack inspection using a Support Vector Machine (SVM) classifier optimised with a Genetic Algorithm (GA). The system integrated image and ultrasonic sensors to capture surface and subsurface crack features. Image features, such as angular second moment, contrast, correlation, and entropy, were extracted using the Gray Level Co-occurrence Matrix (GLCM), while ultrasonic features included echo height and echo time, offering depth and internal structure information. A mobile inspection platform with suction cups enabled stable, precise data collection. The GA optimised the SVM by selecting optimal parameters (penalty factor C and kernel parameter σ), improving accuracy to 93.3%, compared to 88.9% with SVM alone and 71.5% with single sensor methods. This dual-sensor fusion approach improved crack detection accuracy, overcoming challenges of low resolution and human error in traditional visual inspections. Implemented in MATLAB, the system demonstrated robustness and adaptability for various defect types, providing a reliable framework for enhanced aircraft maintenance and safety inspections.

In 2017, Malekzadeh et al. [86] proposed an automated aircraft fuselage defect detection system using Deep Neural Networks (DNNs), specifically CNNs pre-trained on ImageNet (AlexNet and VGG-F). This system combined a VGG-F model as a feature extractor with a linear SVM classifier, achieving high performance in defect detection with 96% accuracy, sensitivity, and specificity. The SURF Interest Point Extractor focused on regions of interest (ROI), resulting in a 6× speed-up by only evaluating selected patches. The system processed a 20-megapixel image in 15 s, operating in MATLAB with the MatConvNet library. The dataset consisted of high-resolution RGB images in JPEG format, with data-level balancing through oversampling and undersampling and a binary mask to represent defects. A low-pass Gaussian filter addressed noise in unwashed fuselage images, enhancing defect detection accuracy. This method demonstrated a viable approach to automated, high-accuracy fuselage inspection for aviation maintenance.

Miranda et al. [91] (2019) developed a hybrid model for aircraft defect classification using a combination of ResNet50 CNN and Prototypical Networks to address the extreme class imbalance in UAV-acquired images. This method was designed for detecting various fuselage defects, such as lightning burns, rivet rash, screw rash and paint defects. The model utilised data augmentation and few-shot learning to improve classification accuracy, achieving a precision of 0.97 and recall of 0.77 for rare defects. The study found that, depending on the class and sample size, different machine-learning approaches were suitable, leading to a combined model that applies CNNs to common classes and few-shot learning to rare ones. Implemented in Python with high-resolution UAV images, the approach showed that hybrid models effectively balance performance for both common and underrepresented categories.

In another similar research project, Miranda et al. [33] (2019) presented a UAV-based system for inspecting aircraft exterior screws using advanced computer vision. The UAV employed precise laser-based localisation to position itself relative to the aircraft without GPS, ensuring accurate inspections indoors and outdoors. A CNN with SSD and YOLO models detected screws and identified missing or defective ones. Regions of Interest (ROIs) were selected manually and refined with Generative Adversarial Networks (GANs) and depth maps to enhance pattern matching under various lighting conditions. A 3D model of the aircraft guided the UAV's navigation and camera alignment. Detected screws were matched with expected patterns using a bipartite graph, improving accuracy by referencing a 3D Digital Mock-Up (DMU) of the aircraft. The system achieved over 95% precision and recall, identifying critical defects. For loose screw detection, it analysed screw alignment changes by comparing screw slots with red operator markings.

In 2020, Bouarfa et al. [92] explored automated aircraft maintenance using Mask R-CNN for dent detection. Mask R-CNN's instance segmentation capability enabled precise pixel-level detection, crucial for non-uniform dent shapes. The model, trained with data-augmented images and pre-trained COCO weights, achieved an average precision of 54% and recall of 46%. After additional training, precision increased to 69% and recall to 57%. Photos were sourced from the Abu Dhabi Polytechnic hangar and annotated using VGG Image Annotator. Implemented in Python with libraries like TensorFlow and Keras, this study faced limitations, including a small and varied dataset, which impacted model accuracy. Environmental factors, such as lighting and reflections, also affected detection performance, leading to false positives with elements like rivets and raindrops.

Ren et al. [94] (2020) developed a stacked ensemble model for surface defect detection in aircraft visual inspections. This approach combined three CNN architectures—ResNet18, GoogLeNet, and VGG11_bn—as base learners with a logistic regression meta-learner. The ensemble enhanced classification accuracy by leveraging error diversity among different CNN models, achieving 99.8% accuracy and 100% recall in defect detection, outperforming single-model frameworks. Defects examined included aircraft surface cracks, corrosion, scratches, and gouges. Images were sourced from borescope inspections, and a central region of 672 $\times$ 448 pixels was selected to reduce distortion and lighting issues. Implemented in PyTorch, the model used data augmentation and cross-entropy loss with stochastic gradient descent. This ensemble approach demonstrated improved reliability in automated defect detection, which is crucial for safety-critical systems like aircraft propellers.

In 2022, Avdelidis et al. [95] developed a two-step defect recognition and classification process using deep learning to automate aircraft inspections conducted with UAVs. The system used a DenseNet201 CNN model for defect detection and an ensemble of EfficientNetB1, EfficientNetB5, EfficientNetB4, and DenseNet169 CNN models for defect classification. The ensemble approach was designed to handle a range of defect types, including missing paint, dents, lightning strike damage, and patch repairs, achieving up to 100% accuracy in specific classes (e.g., paint damage and dents) and an overall defect detection accuracy of 81.82%. A custom dataset of high-resolution images (4800 $\times$ 3200 pixels) captured in a maintenance hangar was used, with a semi-automated Python script for selecting regions of interest (ROI) by cropping relevant areas, followed by grayscale conversion to reduce colour dependency. The system was implemented in TensorFlow, utilising transfer learning and data augmentation to mitigate the limitations of a small, imbalanced dataset. Despite these limitations, the approach demonstrated a promising framework for UAV-based defect detection, with high accuracy in detecting and classifying defects critical for aircraft safety.

Ding et al. [96] (2022) proposed an automated pixel-level defect detection method for aircraft skin based on an enhanced Mask Scoring R-CNN. The model integrated a Convolutional Block Attention Module (CBAM) and a feature fusion module to refine feature representation alongside a new classifier head with four convolutional layers. An ablation study showed that the classifier head improved the most, boosting segmentation precision by 12.5% and pixel-level accuracy by 16.98%. The system was tested on a custom dataset of 276 images with aircraft skin defects, achieving 27.66% higher bounding box precision and 20.49% better segmentation precision compared to Mask R-CNN. Additionally, the approach demonstrated robustness in handling low-contrast defects, producing smoother and more accurate segmentation boundaries. This method outperformed existing models, showing its effectiveness in precise and reliable defect detection, which is essential for automated aircraft inspection tasks.

In 2022, Jaeger et al. [97] introduced a deep-learning approach to enhance crack detection in turbine blades using infrared induction thermography. Their method cap-

tured both surface and sub-surface cracks, providing an automated, contact-free solution compared to traditional inspection techniques. The model used ResNet-18 in two configurations: a Large Image Model (LIM) on full-size images and a Small Image Model (SIM) on 64 × 64 cropped patches. SIM focused on high-crack-density areas and achieved an F2-score of 0.85, outperforming LIM's 0.60. To address challenges like data imbalance and small crack size, the authors applied focal loss, oversampling, and data augmentation. The system, implemented with fastai and PyTorch on an NVIDIA RTX 2080 Ti GPU, increased inspection accuracy and efficiency, supporting inspectors in identifying critical turbine blade defects.

Oh et al. [98] (2024) proposed a CNN-based approach for camera pose estimation and image localisation in aircraft inspections. The method used a customised PoseNet model with an Xception backbone. It was fine-tuned on synthetic images generated from a 3D aircraft model. A geometric loss component leveraged the fixed structure of the aircraft to improve accuracy. Tested on real Airbus A320 images, the system achieved localisation errors under 0.24 m and orientation errors below 2°. It operated without external infrastructure or contact with the aircraft, making it suitable for airport use. Domain randomisation varies textures and lighting in synthetic images, enhancing real-world performance. The workflow included camera initialisation, path planning, and image localisation. This approach supported precise, efficient inspections under time constraints in airports.

2.3. Material Selection

In 2022, IATA's Airline Maintenance Cost Executive Commentary provided insights into global Maintenance, Repair, and Overhaul (MRO) spending by aircraft segment [2]. The chart below (Figure 7) shows that most spending in 2022 was directed toward engine and airframe maintenance. Forecasts for 2032 suggest a similar spending pattern, with a slight increase in engine maintenance costs. This reflects the critical focus on engine and airframe upkeep for safe and efficient aircraft operation.

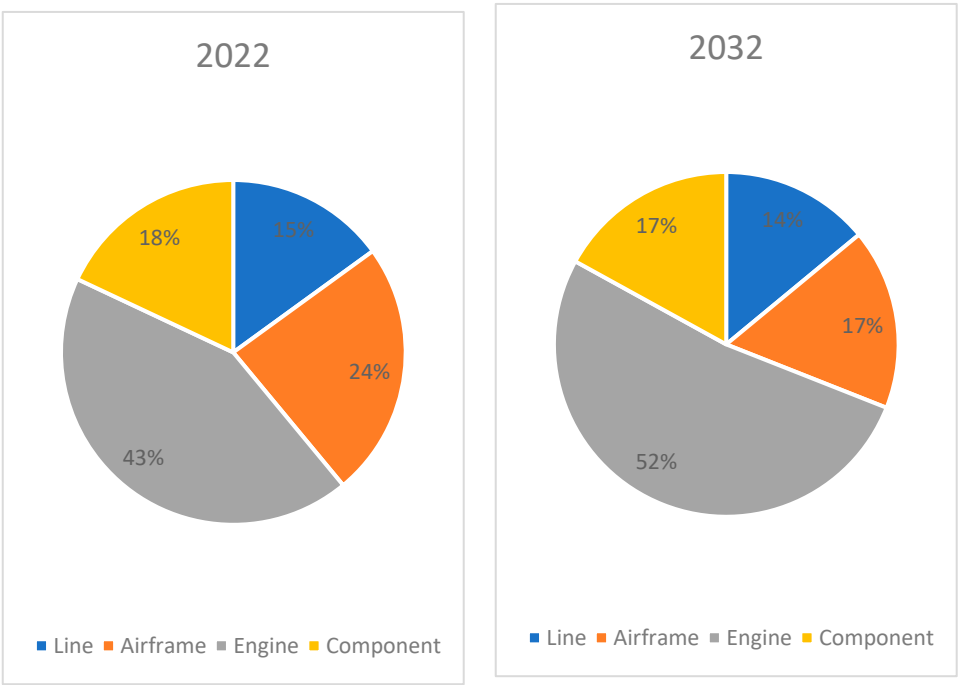

Figure 7. Global MRO Spend by Segment [2].

In the aerospace industry, materials have always played a crucial role in reducing weight, enhancing performance, and improving fuel efficiency. The primary aim is to lower costs while maintaining safety. In this context, Zhang et al. [99] published a paper outlining the material requirements for designing aircraft structures and engines, highlighting the advantages and challenges of current materials, and introducing future trends in aerospace materials. The earliest airframe materials were wooden, with the first flight occurring in 1903. In 1927, aluminium-based alloys dominated aircraft structures for the next 80 years. However, this trend shifted with the rise in composite materials. Figure 8 below illustrates material trends in Boeing aircraft over the years, showing a rapid increase in composite materials and a decrease in aluminium alloys, especially in the Boeing 787.

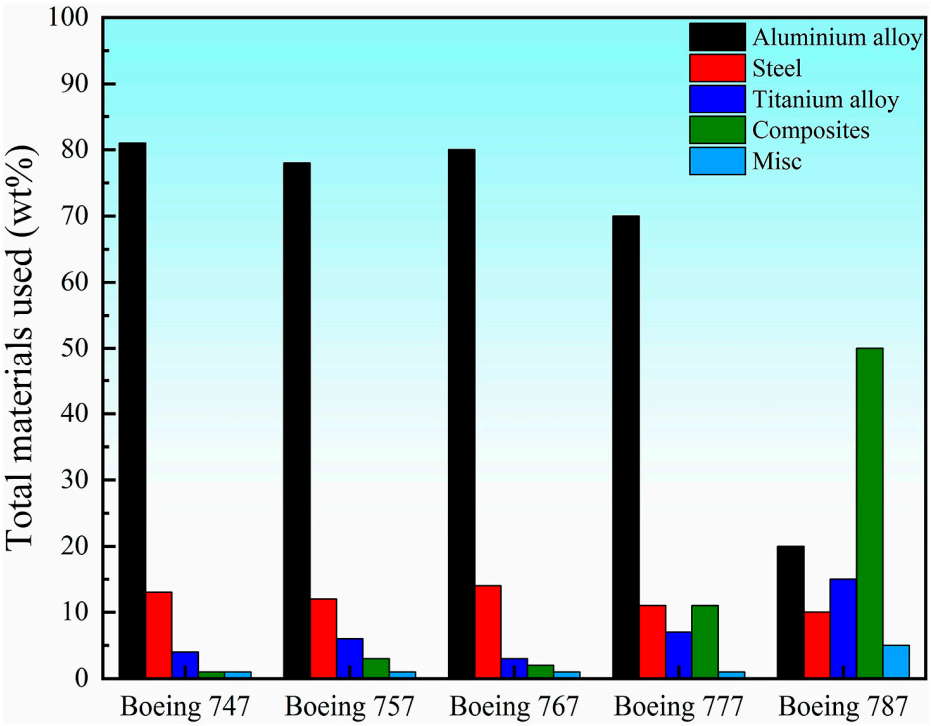

Figure 8. Total materials used in Boeing series aircraft [100].

A similar trend, documented by Muller et al. [101], included data on Airbus aircraft, which have also adopted this shift. As illustrated in Figure 9, in the new generation of Airbus models, there is a notable increase in composite materials and a reduction in aluminium alloys, comprising more than 53% of the Airbus A350. However, aluminium-based alloys continue to play a crucial role in airframe structures and engines due to their cost-effectiveness, ease of manufacturing and their well-known mechanical behaviour. Additionally, these alloys can undergo heat treatment and endure relatively high-stress levels [99].

Several key factors have driven the development of new aircraft materials, such as composite materials, over the past two decades. Increasing payload capacity and extending flight range are top priorities. Improving fuel efficiency and prolonging service life are also essential goals. Reducing the overall weight of the aircraft is critical. Ultimately, these efforts aim to lower operating costs, making modern aircraft more economical and efficient [99]. Before diving into specifics, it is important to define composite materials. Composites are materials made from two or more distinct components that, when combined, offer enhanced properties that the individual materials cannot achieve on their own [102].

Many researchers, including Wong et al. [103] highlighted the benefits of using composite materials in contrast with conventional metallic counterparts. A few examples are weight efficiency, low maintenance, design flexibility and integrity, corrosion resistance and

a lifespan of approximately 28 years. Composite materials are extensively used throughout the aircraft airframe. In the Airbus A380 (Figure 10), for example, composites are incorporated into the centre wing box, horizontal and vertical tailplanes, outer flaps, as well as the unpressurised fuselage and rear pressure bulkhead. These materials also hold great promise for engine components, contributing to further weight reduction and improved performance. The primary types of composites include ceramic matrix, metal matrix, and polymer matrix composites. Of these, polymer matrix composites (PMCs) are the most widely used. Notably, in Boeing 777 and 787 aircraft, PMCs account for up to 50% of their weight, primarily as carbon fibre-reinforced polymers (CFRP). PMCs can be further classified into two subcategories: thermoplastics and thermosets [99].

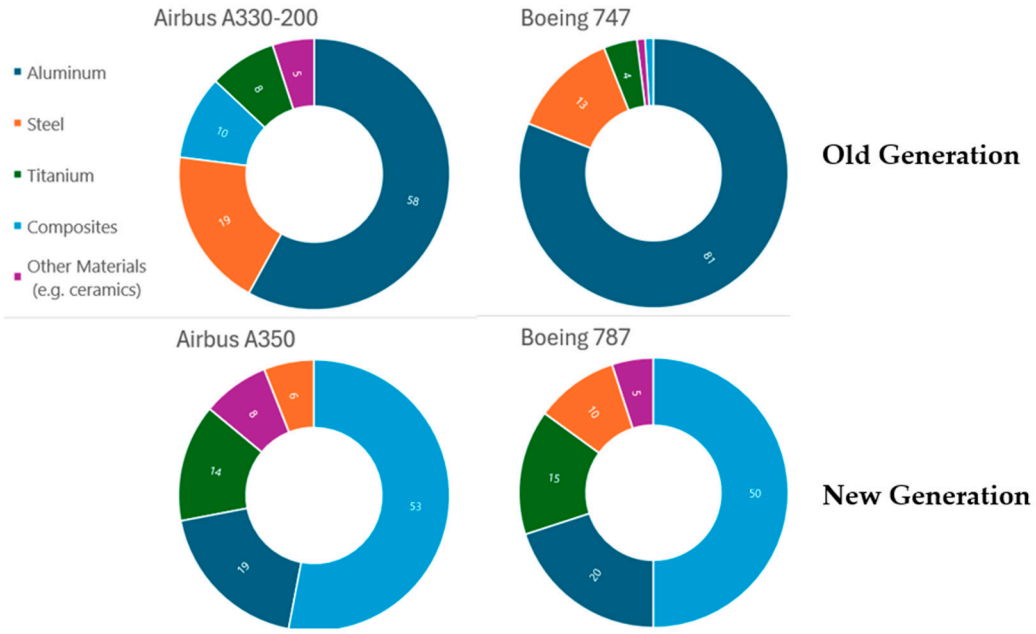

Figure 9. Total materials used in Boeing and Airbus series aircraft [101].

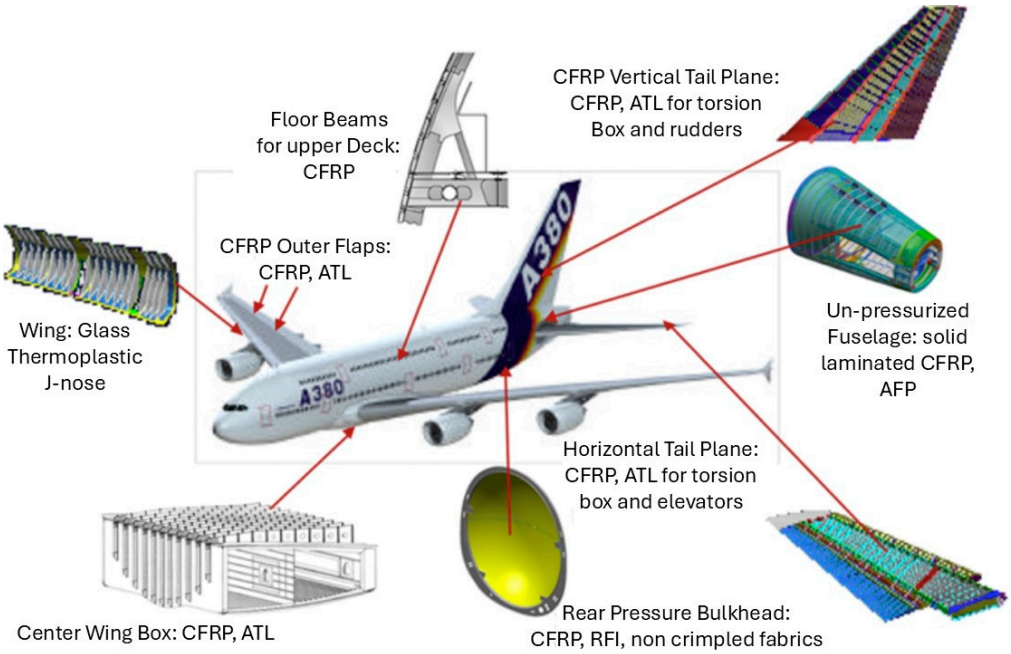

Figure 10. The use of composites in Airbus A380 [104].

The Table 6 below outlines the key material requirements for various aircraft components based on the specific loads and conditions they encounter. The wing, for example, experiences bending forces during flight and additional stresses during take-off and landing. To endure these forces, materials used for the wing must have high tensile and compressive strength, with options including 2024 aluminium alloy and carbon fibre-reinforced polymer composites. The fuselage faces high cabin pressure and shear loads, requiring materials with strong tensile and shear properties, such as aluminium alloys. For high-temperature areas like the exhaust nozzle and aircraft brakes, materials need high heat resistance, with ceramic matrix composites and carbon fibre-reinforced silicon carbide often used. Lastly, control surfaces such as ailerons, flaps, and landing-gear doors require materials with a high strength-to-weight ratio, where both thermoset and thermoplastic polymer matrix composites are effective choices [99].

Table 6. Material requirements and example materials for key aircraft components [99].

Component	Applied Loads/Conditions	Material Requirements	Example Materials
Wing	Subjected to bending during flight; additional loads during taxiing, take-off, and landing; compression on the upper surface and tension on the lower surface during flight	High tensile and compressive strength	2024 Al-based alloy: Moderate yield strength (324 MPa), good fracture toughness (37 MPa $m^{1/2}$), high elongation (21%); Polymer Matrix Composites (PMC) such as CFRP: High strength (3450–4830 MPa), elastic modulus (224–241 GPa), high-temperature resistance (290–345 °C)
Fuselage	Exposed to high cabin pressure and shear loads	High tensile and shear strength	2024 Al-based alloy: Used for moderate yield strength and durability
Exhaust Nozzle	Exposed to high temperatures	High-temperature capability	Ceramic Matrix Composites (CMC)
Aircraft Brakes	Subjected to extremely high temperatures (up to 1200 °C under emergency conditions)	High-temperature resistance	Carbon fibre-reinforced silicon carbide
Ailerons, Flaps, Landing-Gear, Doors	High specific strength and specific modulus needed	Lightweight with high strength-to-weight ratio	Polymer Matrix Composites (PMC): Both thermoset and thermoplastic PMCs

2.4. Type of Defects

This section examines the two most widely used materials in aircraft manufacturing: metallic and composite materials. It explores various types of defects associated with these materials, as investigated by other researchers in the field. The focus is on how these defects impact aircraft maintenance and the methods used to inspect and characterise them.

The Table 7 below summarises typical types of defects found during the manufacturing process or during in-service in aerospace materials, divided into metallic and composite categories. Metallic materials often suffer from issues like fatigue, corrosion, and wear, which weaken their structure. In contrast, composite materials are more sensitive to problems such as delamination, fibre cracking, and impact damage, which affect their layered and bonded nature. This breakdown shows the unique damage challenges faced by each material type.

The table above corresponds to the image below, providing a detailed view of the shape, location, and unique attributes of each defect. This illustration showcases typical material defects found in both composite and metallic structures. Figure 11a represents defects in composite materials, such as impact damage, delamination, porosity, and fibre/matrix cracking. Figure 11b shows a jet engine turbine blade with thermal cracks and delamination between ceramic coatings and CFRP layers. Figure 11c displays honeycomb panel defects,

including core crushing, water ingress, and skin-to-core debonding. Finally, Figure 11d illustrates common issues in metallic components, like voids, corrosion, material inclusions, and both parallel and perpendicular cracks. Together, these diagrams provide a clear visual overview of defect types in aerospace materials.

Table 7. Common Types of Damage in Metallic and Composite Aerospace Materials [105].

Type of Defects During Manufacturing and In-Service	Material	
	Metallic	**Composite**
	❖ Fatigue cracks	❖ Disbonds
	❖ Pores and voids	❖ Delamination
	❖ Corrosion	❖ Foreign Inclusion
	❖ Material inclusions	❖ Fibre/Matrix Cracking
	❖ Welded sheets without metal diffusion	❖ Honeycomb cell wall damage
	❖ Overload	❖ Porosity
	❖ Wear	❖ Thermal stress cracking
	❖ Creep	❖ Fatigue
		❖ Impact damage and BVID
		❖ Water ingress
		❖ Absence of adhesive
		❖ Skin-to-core debonding
		❖ Core crushing

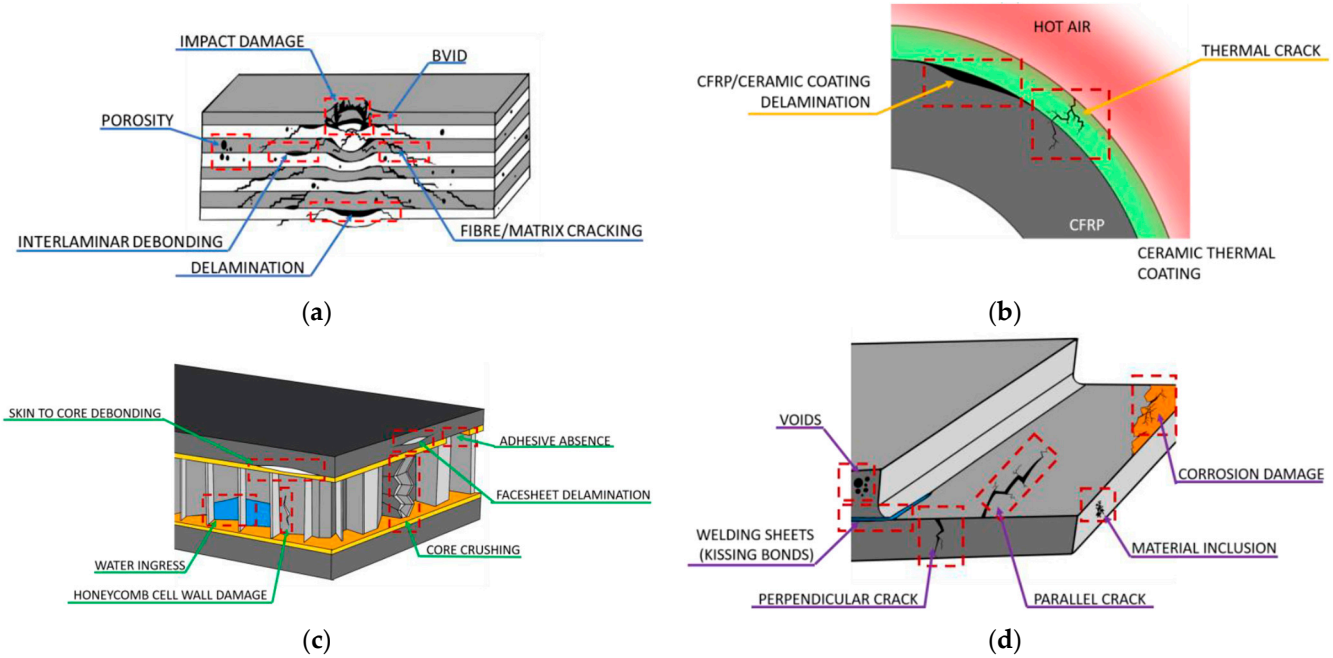

Figure 11. (**a**) Illustration of typical material defects for composite structures; (**b**) jet engine turbine blades; (**c**) honeycomb panels; (**d**) metallic aircraft and spacecraft components [39].

The following sections will analyse three representative examples of fabricated specimens with artificially induced defects to simulate real-world scenarios. Each example includes details on the material type, geometry, defect fabrication methods, and inspection techniques used by researchers.

Lysenko et al. [46] prepared an AD31T5 aluminium alloy specimen with dimensions of 360 mm in length, 120 mm in width, and 5 mm in thickness. The sample included artificial circular defects arranged in various cluster densities, sizes, and configurations. The Figure 12 below shows the specimen, detailing the number of holes and their actual depth values. AD31T5 aluminium alloy is commonly used in the aviation industry for aircraft frames, support structures, and interior fittings due to its strength and corrosion resistance.

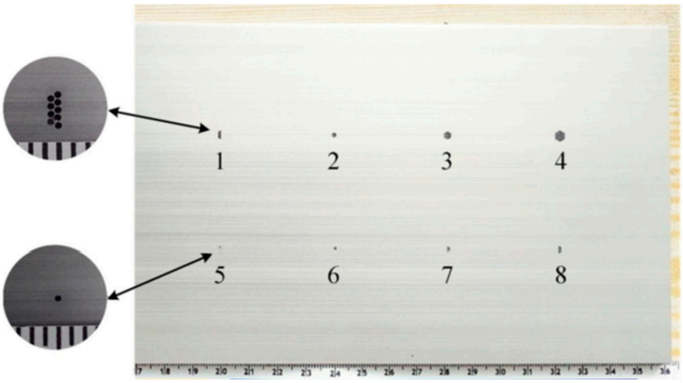

No. of defect	The number of holes n (length in mm)
1	9 (2.9)
2	7 (1.7)
3	19 (2.9)
4	37 (4.1)
5	1 (0.5)
6	3 (1.1)
7	5 (1.7)
8	7 (2.3)

Figure 12. Sample made of AD31T5 alloy [46].

In another study, Zhang et al. [42] employed an autonomous UAV-based ultrasonic system to inspect an aluminium specimen. The researchers created a 1000 mm × 1000 mm × 15 mm aluminium sample with twenty-five flat-bottom holes of various diameters and depths to simulate sub-surface defects.

In the study by Reyno et al. [20], two types of honeycomb sandwich aircraft panels—a flat panel and a curved panel—were fabricated to assess surface damage using 3D scanning technology. These panels were constructed with specific materials: the flat panel utilised Al 7075-T6 for the top face sheet, Al 5052 for the core, and epoxy/fibreglass for the bottom face sheet. On the other hand, the curved panel used Al 2024-T3 for both the top and bottom face sheets, with Al 5052 as the core. Each panel featured a heat-resistant epoxy adhesive for structural integrity. Figure 13a,b display images of the flat and curved panels, respectively, illustrating the setup for dent inspection and the panel geometry. This experiment aimed to simulate real-world damage scenarios and evaluate the precision and reliability of 3D scanning as a non-destructive inspection method.

Flat panel specification

Specification	Value
Top face sheet material	Al 7075-T6
Core material	Al 5052
Bottom face sheet material	Epoxy/fiberglass
Adhesive	Heat-resistant epoxy Hysol EA 934NA
Total panel thickness	12.7mm (0.50 in)
Top face sheet thickness	0.51 mm (0.020 in)

Curved panel specification

Specification	Value
Top face sheet material	Al 2024-T3
Core material	Al 5052
Bottom face sheet material	Al 2024-T3
Adhesive	Heat-resistant epoxy Hysol EA 934NA
Total panel thickness	6.91mm (0.272 in)
Top face sheet thickness	0.51 mm (0.020 in)

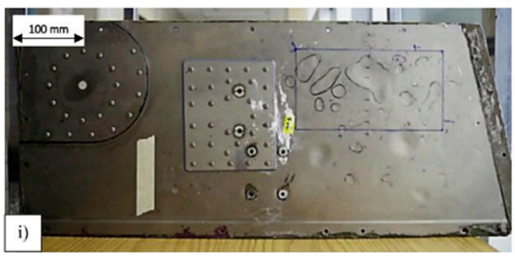

(**a**)

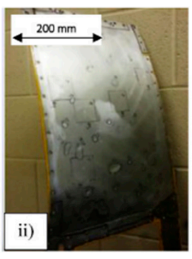

(**b**)

Figure 13. (**a**) Honeycomb sandwich aircraft panel inspection specimens; (**b**) Flat panel Curved panel [20].

2.5. Size and Depth Estimation Techniques

Accurately measuring the depth, width, and length of detected defects in the aviation industry is a complex process. Manual tools, as discussed earlier, have limitations in precision and consistency. Automating this process improves reliability, consistency, and safety. The following section analyses three examples of depth measurement techniques researchers used for various aircraft defects. Additionally, two examples will demonstrate methods to estimate the width and length of detected defects.

As described by Reyno et al. [20] the 3D scanning process was employed to measure dent depths on damaged aircraft panels by comparing the actual panel surface (represented as a 3D point cloud) with an approximated undamaged surface. As illustrated in Figure 14, this undamaged surface was digitally recreated using undisturbed regions of the panel. The comparison was performed using deviation analysis, which calculated dent depths as the perpendicular distance between the two surfaces.

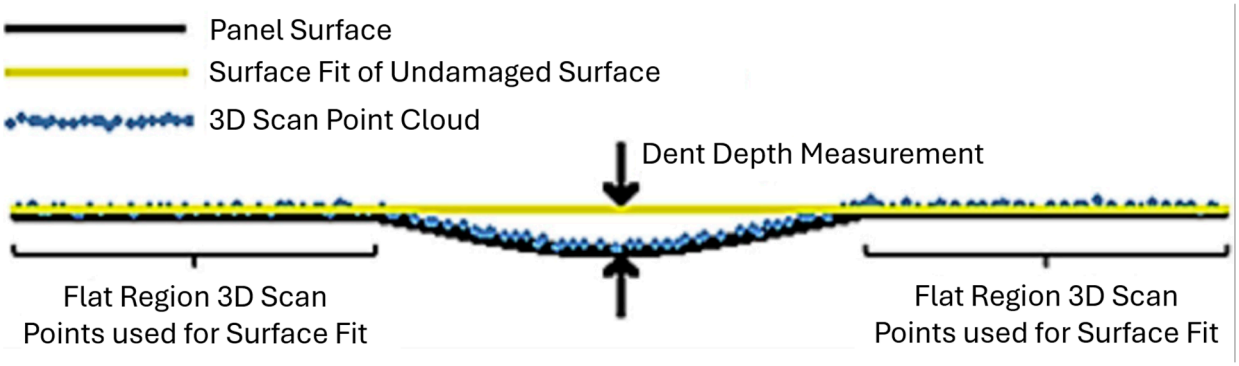

Figure 14. Illustration of the dent depth measurement [20].

The analysis generated a colour map that clearly indicated the extent and depth of the dents. The method demonstrated reliable accuracy, with a maximum deviation of ±0.06 mm for flat panels and ±0.05 mm for curved panels. These results matched closely with measurements taken using traditional manual depth gauges but required significantly less inspection time. Additionally, the method was capable of supporting the detection of Barely Visible Impact Damage (BVID), a critical threshold in aviation maintenance standards.

In another similar study, Jovančević et al. [19] used the above approach to estimate the defect's depth. As shown in Figure 15, the process started by identifying undamaged surface areas. These regions acted as a reference for recreating the original geometry. A Weighted Least Squares (WLS) method was used to fit a smooth quadratic surface to these points, creating the ideal reference surface. The defect depth was then calculated by measuring the vertical difference between the ideal surface and the damaged surface. This difference, Δz, followed the formula:

$$|\Delta z| = \left| z_{P_{\text{ideal}}} - z_{P_{\text{original}}} \right| \quad (1)$$

A colour-coded map highlighted depth variations across the surface. The method achieved high accuracy, with less than 10% error compared to standard measurements.

Another way to estimate the pixel depth is to use photogrammetry and, more specifically, specialised software such as Meshroom [106] using the AliceVision framework, which applies a step-by-step process to calculate pixel depth in a scene. It starts by confirming the positions and angles of cameras using a method called Structure-from-Motion (SfM). This ensures that at least two images of the same area are available for comparison. The next step involves measuring pixel similarities across images using a technique known as Zero-Mean Normalized Cross-Correlation (ZNCC). These measurements help form an initial depth

map that combines local and global data for accuracy. The depth map is then refined by increasing its resolution and fine-tuning depth values through computational adjustments. To remove inaccuracies, the system aligns depth variations with visible features in the images, such as edges. The result is a detailed depth map, which can be visualised in both 2D and 3D.

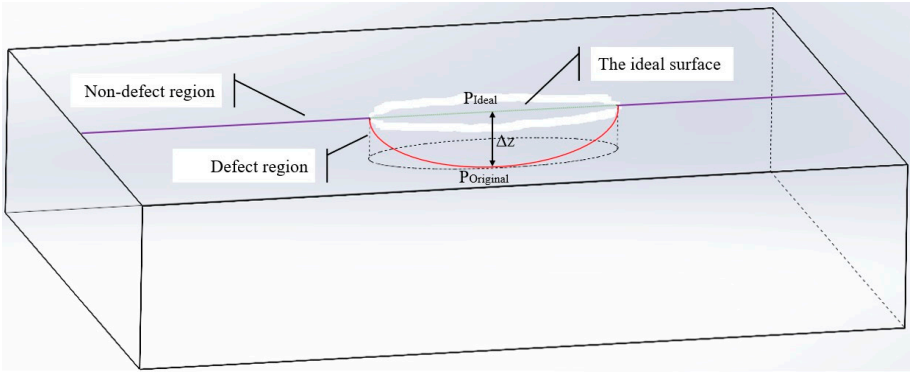

Figure 15. An illustration of the approach for calculating defect depth [19].

In a recent paper, Plastropoulos et al. [35] developed a method to measure defects on aircraft surfaces using UAVs equipped with cameras and LiDAR. It started by capturing images with calibrated camera settings, including focal length, sensor dimensions, and LiDAR-measured distances. Grayscale conversion and Gaussian blurring reduced noise in the images. The method then applied Canny edge detection to identify edges, followed by dilation and erosion operations to refine contours. Pixel distances within defect contours were calculated for measurements like width and height. To convert these pixel dimensions into real-world measurements, the technique relied on similar triangle geometry (please refer to Figure 16).

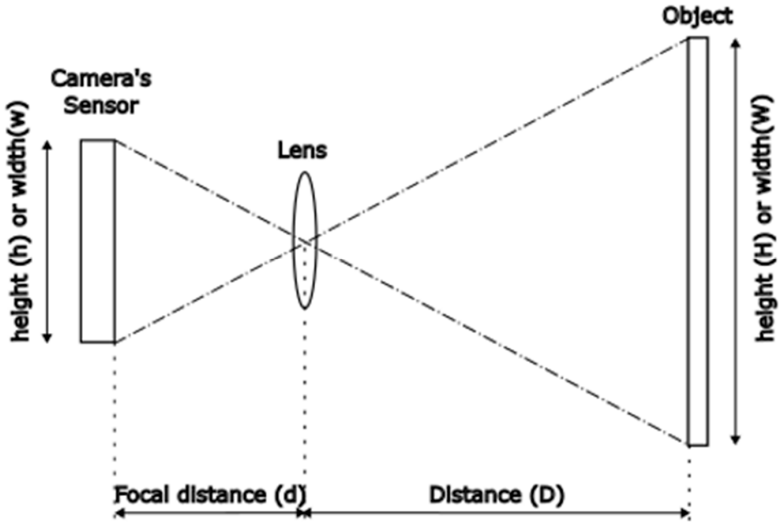

Figure 16. Similar Triangles method to calculate the object's dimensions [35].

The calculations involved key parameters like the focal length (f), sensor width (*sensorw*), image width (*imagew*), and the distance between the camera and the defect (D). Real-world defect width (W) was derived as:

$$W = w \times \frac{D}{f} \quad (2)$$

For more advanced measurements, the method used effective focal length (*EFL*). It related pixel dimensions to real-world size as:

$$defect_w = \frac{D \cdot dA \cdot sensor_w}{f \cdot image_w} = \frac{D \cdot dA}{EFL}, \; where \; EFL = \frac{f \cdot image_w}{sensor_w} \quad (3)$$

Lab tests confirmed high accuracy, but field conditions like reflective surfaces and non-perpendicular imaging introduced challenges. Despite these, the approach provided a reliable framework for automated defect measurement with potential refinements.

Reyno et al. [20] as illustrated in Figure 17, measured the dent depth and also analysed the dent length and area through a step-by-step process. They performed a deviation analysis in Design X software with the colour bar set to a solid colour. This created a colour map that outlined the dent perimeter. Deviations beyond a set tolerance appeared in a single colour, such as dark blue, making them easy to identify. The team converted the colour map into an 8-bit grayscale image using ImageJ software. They noted that sharpening or despeckling could reduce noise but did not apply these in their study. For curved surfaces, they used the Design X Normal To Function to adjust the 3D CAD surface. This ensured that the map aligned perpendicularly with the viewer for accurate measurements. Based on dimensional data from Design X, they defined a unit scale in pixels per millimetre and calculated dent parameters, including area and maximum length, in ImageJ. This method provided accurate measurements for simple and complex dents on flat and curved panels, offering a detailed view of the damage.

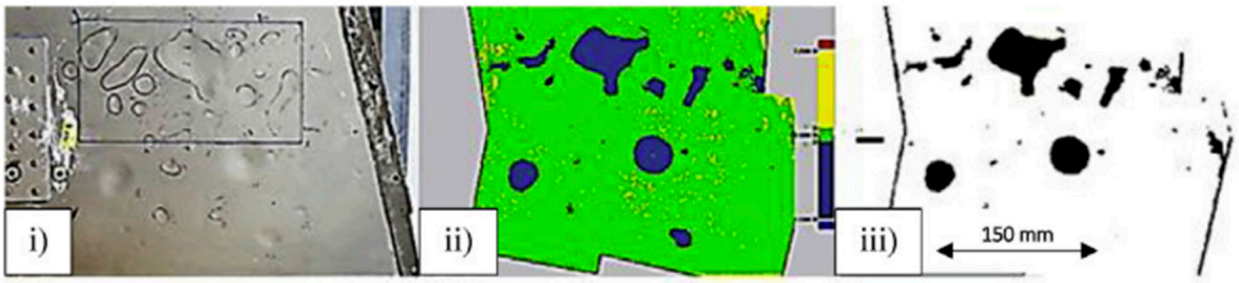

Figure 17. Dent length and area estimation—colour map and measurements in greyscale [20].

3. Discussion

The comparative evaluation of non-destructive testing (NDT) technologies presented in Table 8 was systematically derived from the literature review conducted in the previous sections. This assessment was based on predefined performance criteria, including defect detection accuracy, consistency, ease of use, acquisition speed, portability, and cost-effectiveness. The data for this comparative analysis were extracted from multiple sources, including empirical studies, experimental evaluations, and industry reports, ensuring a balanced and evidence-based comparison of the technologies.

Each parameter in the table weighs one, indicating the presence of a given characteristic for the NDT methods. Including one value for a specific parameter signifies that the technology effectively meets the corresponding performance criterion. This uniform scoring approach ensures objectivity in comparing the strengths and limitations of each method without introducing weighted biases. The most suitable NDT techniques for automated aircraft inspection were identified by analysing these parameters collectively. The results of this comparative analysis highlight that Infrared Thermography (IRT) combined with Photogrammetry emerges as the most suitable NDT technique for the objectives of this research.

Table 8. Proposed parameters to evaluate the performance of non-destructive technologies ('X' indicates that the corresponding NDT technology meets the described criteria. Blank spaces indicate that the technology is not suitable for the given parameter).

Criteria	Sub-Criteria	Parameters	NDT Technologies									
										3D Scanning		
			X-Ray	Ultrasonic	Magnetic Particle	Penetrant	Eddy Current	Acoustic Emission	IRT	Laser	LiDAR	Photogrammetry (RGB)
Capability	Surface defects	Cracks		X	X		X	X	X			
		Surface-Opening				X			X	X	X	X
		Corrosion							X			
		Impact								X	X	X
		Damage								X	X	X
		Dents								X	X	X
		Surface Wear										
		Surface Deformation										
	Near-surface defects	Cracks		X	X		X	X	X			
		Debonding	X	X				X	X			
		Corrosion							X			
		Impact							X			
		Damage		X				X	X			
		Delamination										
	Non-Contact Inspection	No-coupling agent required	X	Requires a coupling medium (gel, water, or oil)	Requires magnetic ink or powder application	Requires liquid penetrant and developer application	Requires probe contact with the material	Needs direct contact with the structure	X	X	X	X
Performance under different environments	Efficiency under different finishes	High defect detection capability under different materials	X Metals, composites, ceramics	X Metals, composites, some plastics	Only ferromagnetic materials	Only materials with smooth surfaces	Conductive materials only	X Metals, composites, some ceramics	X Metals, composites, plastics	X Most materials	Most solid structures	X All visible materials
	Consistency	Repeatability	X	X	Manual application only	Depends on surface preparation, dwell time, and lighting	X	Depends on sensor placement and background noise	Environmental factors	X	X	X
	Sensitivity	High defect detection accuracy	X	X	X	X	X	X	X	X	X	X
		High coverage range	Requires multiple exposures	Requires manual scanning	Only works in localised areas	Requires individual component inspection	Limited to small probe areas	X	X	Moderate coverage range	X	X

Table 8. *Cont.*

Criteria	Sub-Criteria	Parameters	NDT Technologies								
									3D Scanning		
			X-Ray	Ultrasonic	Magnetic Particle	Penetrant	Eddy Current	Acoustic Emission	IRT	Laser	LiDAR	Photogrammetry (RGB)
Ease of use	Ease of data collection	Portability	Heavy equipment, shielding is required	X	X	X	X	X	X	X	X	X
Ease of use	Ease of data collection	Minimum safety requirements	Radiation hazard requires shielding and legal permits	X	X	Uses chemicals that require proper ventilation	X	X	X	X	X	X
	Ease of data analysis	Minimum complexity of data analysis	Requires trained personnel to interpret images	X	X	X	X	Complex waveform analysis requires signal processing and pattern recognition	X	X	X	X
Cost	Data collection cost	Low equipment and software cost	Requires expensive equipment, protective shielding, and specialised software	Advanced phased-array systems cost more	X	X	X Interpretation software can add cost	It needs multiple sensors and advanced signal-processing software	X	High-precision versions are costly	X More expensive than photogramme-try	X
Speed	Data collection speed	High acquisition speed	Requires exposure time + processing time	Single-probe scanning takes time	X	Requires dwell time for the penetrant to seep into defects	X	X	X	Scanning large surfaces takes time	X	X
Speed	Data analysis speed	Data analysis is quick and efficient	Requires image processing, defect interpretation, and expert review	X	X	X	X	Requires signal processing and pattern analysis	X	Requires point cloud processing	Large datasets require software processing	Post-processing takes time
TOTAL SCORE			5	11	9	6	10	10	18	11	13	14

This research has the potential to make significant intellectual contributions to the field of aircraft inspection by advancing automated methods for structural evaluation. An essential contribution is developing a novel inspection system that combines 2D RGB and infrared thermal images with their corresponding 3D models, using photogrammetry to detect surface and near-surface defects in both metallic and composite aircraft materials. This non-contact approach improves defect detection accuracy compared to traditional methods and reduces aircraft downtime and operational costs. Additionally, integrating photogrammetry with infrared thermal and RGB cameras expands the capabilities of non-destructive testing (NDT) techniques, enabling comprehensive 3D reconstructions and more detailed analyses of defect characteristics. To the best of my knowledge, this is the first application of combining advanced cameras with photogrammetry for 3D inspection in the aviation industry. However, similar technology has been successfully used in fields like forensic science, civil infrastructure, and archaeology. Furthermore, many researchers have encountered challenges with unbalanced datasets during machine learning model training due to the absence of open-source datasets containing aircraft defects and the difficulty of accessing aircraft specimens because of intellectual property restrictions and protections enforced by OEMs. Using synthetic images generated from 3D models, combined with real images, offers a valuable solution to these challenges. Finally, integrating all these technologies into a single graphical user interface (GUI) makes the solution user-friendly and accessible to operators without requiring expertise in the field.

The findings from this research could have important potential impacts on both the aviation and machine learning industries. In aviation, this approach can offer a more accurate, efficient, and non-invasive method for detecting defects in aircraft materials, which could drastically reduce maintenance costs and aircraft downtime. It can also improve reliability and safety and minimise human error. While this research focuses on smaller-scale aircraft specimens, demonstrating the effectiveness of this technology opens the door to scaling up. Using a UAV system instead of a robotic arm, aircraft maintenance companies can extend these inspection methods to larger aircraft components. For the machine learning industry, an open-source dataset that consists of 2D images and 3D models will be available to other researchers and individuals for further use. Moreover, utilising both real and synthetic data addresses the common challenge of unbalanced datasets, improving the accuracy and robustness of defect detection algorithms. The GUI and all the developed libraries will also be open-source and available through GitHub. Finally, the sophisticated machine learning techniques will be more accessible to the research and aviation community, encouraging further innovation.

Automated Non-Destructive Testing (NDT) methods, such as Infrared Thermography (IRT) and Photogrammetry, offer advantages. However, implementing these technologies in real-world applications comes with challenges. One major obstacle is cost, as high-resolution IRT cameras, photogrammetry tools, and advanced processing software require a significant initial investment. Integrating automated NDT systems into existing maintenance workflows can also be complex due to compatibility issues with industry standards and regulatory requirements. Another challenge is training personnel since shifting from traditional NDT methods to automated systems requires expertise in image analysis, defect identification, and software operation. Without proper training, inspection accuracy could suffer. Regular maintenance, including sensor calibration, software updates, and system adjustments, is also necessary to keep the equipment running reliably.

Several strategies can help address these challenges. A cost–benefit analysis can demonstrate how automated NDT systems save money over time by speeding up inspections and minimising aircraft downtime. Modular system designs could make implementation easier by allowing gradual upgrades instead of requiring a significant upfront

investment. To bridge the skills gap, collaboration between industry and academia can provide training programmes and certification courses for NDT professionals. Online learning platforms and augmented reality (AR) tools can further support remote learning. Lastly, predictive maintenance strategies, such as AI-based condition monitoring, can enhance system reliability and reduce unexpected failures. These solutions can make automated NDT technologies more practical, improving efficiency and safety in aviation.

Overall, this work advances current NDT practices and sets new standards that can be applied to improve industrial inspection processes.

4. Conclusions

The increasing demand for automated aircraft inspection and maintenance has led to significant advancements in Non-Destructive Testing (NDT) techniques, machine learning-based defect detection, and automated defect characterisation. This review investigated the latest research developments, emphasising how deep learning, advanced sensor fusion, and real-time automation transform aircraft maintenance practices.

Recent studies demonstrate that AI-driven inspection systems achieve higher accuracy, improved defect classification, and reduced inspection time, mainly through hybrid models, transfer learning, and sensor fusion techniques. Advances in robotics, UAV-based inspection, and deep-learning-enhanced thermography have further improved the efficiency and reliability of damage assessment in metallic and composite aircraft structures. However, challenges remain in areas such as data limitations, environmental factors affecting imaging accuracy, and the need for standardised defect detection datasets.

Future research should focus on expanding high-quality datasets, integrating real-time AI-powered analysis, and improving explainability in deep learning models to enhance trust in automated inspections. Developing self-adaptive defect monitoring systems could further streamline predictive maintenance and aircraft structural health monitoring. The aviation industry is progressing toward more efficient, reliable, and scalable aircraft maintenance solutions by bridging the gap between AI, advanced imaging, and aerospace engineering.

5. Future Directions

This research aims to develop an automated vision-based damage evaluation system capable of detecting and characterising defects in metallic and composite aircraft specimens by analysing 3D data acquired using both an RGB camera and an infrared thermal camera through photogrammetry.

The respective scientific objectives of the research are:

1. To develop a dataset comprising at least 1000 real and 500 synthetic images derived from the 3D model, ensuring it adheres to deep learning standards for accuracy, diversity, and quality.
2. To train and develop a machine learning model capable of detecting and classifying the most common defects for each material, achieving a minimum precision of 80%, a recall of 70%, and an F1 score of at least 0.75.
3. To address the challenges an unbalanced dataset poses and enhance the model's performance by at least 5% by applying advanced imaging techniques.
4. To develop a defect measurement tool capable of estimating the size and depth of the detected defect with an error rate below 10%.

Author Contributions: Conceptualisation, N.P.A.; methodology, K.B., N.P.A. and H.F.; investigation, All Authors; resources, N.P.A. and H.F.; writing—original draft preparation, K.B.; writing—review and editing, All Authors; supervision, N.P.A. and H.F.; funding acquisition, N.P.A. All authors have read and agreed to the published version of the manuscript.

Funding: This research was supported and funded by the British Engineering and Physical Sciences Research Council (EPSRC), grant number EP/T518104/1.

Institutional Review Board Statement: Not applicable.

Informed Consent Statement: Not applicable.

Data Availability Statement: The original contributions presented in the study are included in the article, further inquiries can be directed to the corresponding author.

Acknowledgments: H.F. is grateful for the support provided by the Brazilian National Council for Scientific and Technological Development (CNPq).

Conflicts of Interest: The authors declare no conflicts of interest.

References

1. Scavini, J. File:Boeing 737-800 v1.0.png. 30 October 2011. Available online: https://commons.wikimedia.org/wiki/File:Boeing_737-800_v1.0.png (accessed on 6 February 2025).
2. IATA Maintenance Cost Technical Group. Airline Maintenance Cost Executive Commentary FY2022 Data. February 2024. Available online: https://www.iata.org/en/services/data/safety/gadm/mcx/ (accessed on 30 December 2024).
3. Inmarsat and Cranfield University. Why the Future of Aviation Starts with Connectivity. March 2022. Available online: https://www.inmarsat.com/en/news/latest-news/aviation/2022/technology-innovations-revolutionise-aviation-cranfield-inmarsat.html (accessed on 22 July 2024).
4. Cazzato, D.; Olivares-Mendez, M.A.; Sanchez-Lopez, J.L.; Voos, H. Vision-Based Aircraft Pose Estimation for UAVs Autonomous Inspection without Fiducial Markers. In Proceedings of the 45th Annual Conference of the IEEE Industrial Electronics Society (IECON), Lisbon, Portugal, 14–17 October 2019. [CrossRef]
5. Olaganathan, R. Human Factors in Aviation Maintenance: Understanding Errors, Management, and Technological Trends. *Glob. J. Eng. Technol. Adv.* **2024**, *18*, 92–101. [CrossRef]
6. National Transportation Safety Board. Loss of Pitch Control During Takeoff, Air Midwest Flight 5481, Raytheon (Beechcraft) 1900D, N233YV. Charlotte, North Carolina. January 2003. Available online: https://www.ntsb.gov/investigations/AccidentReports/Reports/AAR0401.pdf (accessed on 30 December 2024).
7. Prasad, V.S.K. A Case Analysis of Human Factors Affecting Aviation Maintenance Personnel. *Int. J. Aviat. Aeronaut. Aerosp.* **2024**, *9*, 123–134. [CrossRef]
8. Aircraft Accident Investigation Commission. Final Report on the Accident of ATR72/212A Version 500 (Registration: 9N-ANC) That Occurred on 15 January 2023, near Pokhara International Airport. 2023. Available online: https://www.tourism.gov.np/files/1/9N-ANC%20FINAL%20Report.pdf (accessed on 5 February 2025).
9. Australian Transport Safety Bureau. Foreign Object Debris Event Involving Airbus A380, VH-OQI. 2024. Available online: https://www.atsb.gov.au/sites/default/files/2024-11/AO-2024-006%20Final.pdf (accessed on 5 February 2025).
10. Civil Aviation Authority. Aircraft Maintenance Incident Analysis. 2016. Available online: https://www.caa.co.uk/our-work/publications/documents/content/cap1367/ (accessed on 30 December 2024).
11. Folkard, S.; Rhythms, B.; Shiftwork Centre, Department of Psychology, University of Wales. Work Hours of Aircraft Maintenance Personnel–CAA PAPER 2002/06. 2003. Available online: https://www.caa.co.uk/our-work/publications/documents/content/caa-paper-200206/ (accessed on 30 December 2024).
12. Wang, Y.; Gogu, C.; Binaud, N.; Bes, C.; Haftka, R.T.; Kim, N.-H. Predictive airframe maintenance strategies using model-based prognostics. *Proc. Inst. Mech. Eng. Part G J. Aerosp. Eng.* **2018**, *232*, 690–709. [CrossRef]
13. Salto¡lu, R.; Humaira, N.; Inalhan, G. Aircraft Scheduled Airframe Maintenance and Downtime Integrated Cost Model. *Adv. Oper. Res.* **2016**, *2016*, 2576825. [CrossRef]
14. Wang, Y.; Gogu, C.; Binaud, N.; Bes, C. Comparing Structural Airframe Maintenance Strategies Based on Probabilistic Estimates of the Remaining Useful Service Life. November 2021. Available online: https://hal.science/hal-03446462 (accessed on 30 December 2024).
15. Sadasivan, S.; Greenstein, J.S.; Gramopadhye, A.K.; Duchowski, A.T. Use of Eye Movements as Feedforward Training for a Synthetic Aircraft Inspection Task. In Proceedings of the SIGCHI conference on Human factors in computing systems, Portland, OR, USA, 2–7 April 2005. [CrossRef]

16. Papa, U.; Ponte, S. Preliminary Design of an Unmanned Aircraft System for Aircraft General Visual Inspection. *Electronics* **2018**, *7*, 435. [CrossRef]
17. US Department of Transportation–Federal Aviation Administration. Visual Inspection for Aircraft. In *Advisory Circular (AC)*; AC 43–204; US Department of Transportation–Federal Aviation Administration: Washington, DC, USA, 1997; pp. 1–236.
18. Civil Aviation Authority. CAP 562: Civil Aircraft Airworthiness Information and Procedures, Issue 8, Amendment 1. April 2022. Available online: https://www.caa.co.uk/publication/pid/92 (accessed on 26 July 2024).
19. Jovančević, I.; Pham, H.-H.; Orteu, J.-J.; Gilblas, R.; Harvent, J.; Maurice, X.; Brèthes, L. 3D Point Cloud Analysis for Detection and Characterization of Defects on Airplane Exterior Surface. *J. Nondestr. Eval.* **2017**, *36*, 74. [CrossRef]
20. Reyno, T.; Marsden, C.; Wowk, D. Surface Damage Evaluation of Honeycomb Sandwich Aircraft Panels Using 3D Scanning Technology. *NDT E Int.* **2018**, *97*, 11–19. [CrossRef]
21. ASamarathunga, A.I.; Piyasundara, N.; Wanigasooriya, A.I.; Kumara, B.S.; Vithanage, V.P.; Chathuranga, D.S. A Robotic Platform for Aircraft Composite Structure Inspection Using Thermography. *Robotics* **2022**, *11*, 62. [CrossRef]
22. DiLaura, D.; Houser, K.; Mistrick, R.; Steffy, G. *The IES Lighting Handbook*, 10th ed.; Illuminating Engineering Society: New York, NY, USA, 2011.
23. Rice, M.; Li, L.; Ying, G.; Wan, M.; Lim, E.T.; Feng, G.; Ng, J.; Jin-Li, M.N.T.; Babu, V.S. Automating the Visual Inspection of Aircraft. In Proceedings of the Singapore Aerospace Technology and Engineering Conference (SATEC), Singapore, 7 February 2018.
24. Drury, C.G.; Watson, J. *Good Practices in Visual Inspection: Human Factors in Aviation Maintenance—Phase Nine, Progress Report*; Applied Ergonomics Group Inc: Madison, IL, USA, 2002.
25. Hobbs, A. An Overview of Human Factors in Aviation Maintenance. Aviation Research and Analysis Report AR-2008-055. December 2008. Available online: https://www.atsb.gov.au/publications/2008/ar2008055 (accessed on 15 August 2024).
26. Dalton, R.P.; Cawley, P.; Lowe, M.J.S. The Potential of Guided Waves for Monitoring Large Areas of Metallic Aircraft Fuselage Structure. *J. Nondestruct. Eval.* **2001**, *20*, 29–46. [CrossRef]
27. Bauda, M.-A.; Bazot, C.; Larnier, S. Real-time ground marking analysis for safe trajectories of autonomous mobile robots. In Proceedings of the2017 IEEE International Workshop of Electronics, Control, Measurement, Signals and their Application to Mechatronics (ECMSM), Donostia, Spain, 24–26 May 2017.
28. Futterlieb, M. Vision-Based Navigation in a Dynamic Environment. LAAS-CNRS, Toulouse, France. 2017. Available online: https://laas.hal.science/tel-01624233v2 (accessed on 30 December 2024).
29. Lakrouf, M.; Larnier, S.; Devy, M.; Achour, N. Moving Obstacles Detection and Camera Pointing for Mobile Robot Applications. In Proceedings of the ICMRE 2017, 2017 3rd International Conference on Mechatronics and Robotics Engineering, Paris, France, 14 September 2017; p. 10.
30. Futterlieb, M.; Cadenat, V.; Sentenac, T. A Navigational Framework Combining Visual Servoing and Spiral Obstacle Avoidance Techniques. In Proceedings of the2014 11th International Conference on Informatics in Control, Automation and Robotics (ICINCO), Vienna, Austria, 1–3 September 2014.
31. Frejaville, J.; Larnier, S.; Vetault, S. Localisation à partir de données laser d'un robot naviguant autour d'un avion. In Proceedings of the Reconnaissance de Formes et Intelligence Artificielle, Clermont-Ferrand, France, 18 June 2016.
32. Toman, R.; Rogala, T.; Synaszko, P.; Katunin, A. Robotized Mobile Platform for Non-Destructive Inspection of Aircraft Structures. *Appl. Sci.* **2024**, *14*, 10148. [CrossRef]
33. Miranda, J.; Larnier, S.; Herbulot, A.; Devy, M. UAV-Based Inspection of Airplane Exterior Screws with Computer Vision. 2019. Available online: https://laas.hal.science/hal-02065284 (accessed on 30 December 2024).
34. Claybrough, M. System and Method for Automatically Inspecting Surfaces. WO 2016/203151 A1, 22 December 2016.
35. Plastropoulos, A.; Bardis, K.; Yazigi, G.; Avdelidis, N.P.; Droznika, M. Aircraft Skin Machine Learning-Based Defect Detection and Size Estimation in Visual Inspections. *Technologies* **2024**, *12*, 158. [CrossRef]
36. Alexakis, E.; Delegou, E.T.; Lampropoulos, K.C.; Apostolopoulou, M.; Ntoutsi, I.; Moropoulou, A. NDT as a monitoring tool of the works progress and the assessment of materials and rehabilitation interventions at the Holy Aedicule of the Holy Sepulchre. *Constr. Build. Mater.* **2018**, *189*, 512–526. [CrossRef]
37. Qu, Z.; Jiang, P.; Zhang, W. Development and application of infrared thermography non-destructive testing techniques. *Sensors* **2020**, *20*, 3851. [CrossRef] [PubMed]
38. Torbali, M.E.; Zolotas, A.; Avdelidis, N.P. A State-of-the-Art Review of Non-Destructive Testing Image Fusion and Critical Insights on the Inspection of Aerospace Composites towards Sustainable Maintenance Repair Operations. *Appl. Sci.* **2023**, *13*, 2732. [CrossRef]
39. Ciampa, F.; Mahmoodi, P.; Pinto, F.; Meo, M. Recent advances in active infrared thermography for non-destructive testing of aerospace components. *Sensors* **2018**, *18*, 609. [CrossRef]
40. Thulasy, T.N.; Nohuddin, P.N.E.; Nusyirwan, I.F.; Hijazi, M.H.A.; Zahra, M.M.A. Application of 3D scanning technology in Royal Malaysian Air Force Industrial Revolution 4.0-based aircraft maintenance. *IET Netw.* **2022**, *11*, 62–67. [CrossRef]

41. Le Reun, A.; Subrin, K.; Dubois, A.; Garnier, S. Improving accuracy reconstruction of parts through a capability study: A methodology for X-ray Computed Tomography Robotic Cell. *Rob. Auton. Syst.* **2023**, *164*, 104564. [CrossRef]
42. Zhang, D.; Watson, R.; Dobie, G.; Macleod, C.; Pierce, G. Autonomous ultrasonic inspection using unmanned aerial vehicle. In Proceedings of the 2018 IEEE International Ultrasonics Symposium (IUS), Kobe, Japan, 22–25 October 2018. [CrossRef]
43. Kikechi, B.M. *Evaluation of Effectiveness of Non-Destructive Testing Techniques for Inspection of Critical Aircraft Components: A Case of the Kenyan Aviation Industry*; University of Nairobi: Nairobi, Kenya, 2020.
44. Luk, B.L.; Chan, H.S. Human Factors and Ergonomics in Dye Penetrant and Magnetic Particles Nondestructive Inspection Methods. 2007. Available online: https://www.engineeringletters.com/issues_v15/issue_1/EL_15_1_25.pdf (accessed on 30 December 2024).
45. Tzitzilonis, V.; Malandrakis, K.; Fragonara, L.Z.; Domingo, J.A.G.; Avdelidis, N.P.; Tsourdos, A.; Forster, K. Inspection of Aircraft Wing Panels Using Unmanned Aerial Vehicles. *Sensors* **2019**, *19*, 1824. [CrossRef]
46. Lysenko, I.; Kuts, Y.; Uchanin, V.; Mirchev, Y.; Levchenko, O. Evaluation of Eddy Current Array Performance in Detecting Aircraft Component Defects. *Trans. Aerosp. Res.* **2024**, *275*, 1–9. [CrossRef]
47. Holford, K.M.; Eaton, M.J.; Hensman, J.J.; Pullin, R.; Evans, S.L.; Dervilis, N.; Worden, K. A new methodology for automating acoustic emission detection of metallic fatigue fractures in highly demanding aerospace environments: An overview. *Prog. Aerosp. Sci.* **2017**, *90*, 1–11. [CrossRef]
48. Sfarra, S.; Ibarra-Castanedo, C.; Avdelidis, N.P.; Genest, M.; Bouchagier, L.; Kourousis, D.; Tsimogiannis, A.; Anastassopoulous, A.; Bendada, A.; Maldague, X.; et al. A comparative investigation for the nondestructive testing of honeycomb structures by holographic interferometry and infrared thermography. *J. Phys. Conf. Ser.* **2010**, *214*, 012071. [CrossRef]
49. Montesano, J.; Fawaz, Z.; Bougherara, H. Use of infrared thermography to investigate the fatigue behavior of a carbon fiber reinforced polymer composite. *Compos. Struct.* **2013**, *97*, 76–83. [CrossRef]
50. Alhammad, M.; Avdelidis, N.P.; Castanedo, C.I.; Maldague, X.; Zolotas, A.; Torbali, E.; Genest, M. Multi-label classification algorithms for composite materials under infrared thermography testing. *Quant. Infrared Thermogr. J.* **2022**, *21*, 3–29. [CrossRef]
51. Eshkalak, S.K.; Ghomi, E.R.; Dai, Y.; Choudhury, D.; Ramakrishna, S. The role of three-dimensional printing in healthcare and medicine. *Mater. Des.* **2020**, *194*, 108940. [CrossRef]
52. Aimar, A.; Palermo, A.; Innocenti, B. The Role of 3D Printing in Medical Applications: A State of the Art. *J. Healthc. Eng.* **2019**, *2019*, 5340616. [CrossRef]
53. Skublewska-Paszkowska, M.; Milosz, M.; Powroznik, P.; Lukasik, E. 3D technologies for intangible cultural heritage preservation—Literature review for selected databases. *Herit. Sci.* **2022**, *10*, 3. [CrossRef]
54. Wits, W.W.; García, J.R.R.; Becker, J.M.J. How additive manufacturing enables more sustainable end-user maintenance, repair and overhaul (MRO) strategies. *Procedia CIRP* **2016**, *40*, 693–698. [CrossRef]
55. Morze, N.V.; Varchenko-Trotsenko, L.O.; Tiutiunnyk, A.V. Introduction of STEAM Education with the Use of 3D Technologies: Modelling, Scanning and Printing. 2016. Available online: https://elibrary.kubg.edu.ua/id/eprint/16224/ (accessed on 30 December 2024).
56. Tofail, S.A.M.; Koumoulos, E.P.; Bandyopadhyay, A.; Bose, S.; O'Donoghue, L.; Charitidis, C. Additive manufacturing: Scientific and technological challenges, market uptake and opportunities. *Mater. Today* **2018**, *21*, 22–37. [CrossRef]
57. Javaid, M.; Haleem, A.; Pratap, S.R.; Suman, R. Industrial perspectives of 3D scanning: Features, roles and it's analytical applications. *Sens. Int.* **2021**, *2*, 100114. [CrossRef]
58. Warwick, G. Lidar Advances as Sensor for Commercial Aviation. Aviation Week Network. 2017. Available online: https://aviationweek.com/aerospace/lidar-advances-sensor-commercial-aviation (accessed on 30 December 2024).
59. Boehler, W.; Vicent, M.B.; Marbs, A. Investigating Laser Scanner Accuracy. In Proceedings of the CIPA 2003 XIXth International Symposium, Antalya, Turkey, 30 September–4 October 2003.
60. Vosselman, G.; Maas, H.-G. *Airborne and Terrestrial Laser Scanning*; Whittles Publishing: Boca Raton, FL, USA, 2010.
61. Westoby, M.J.; Brasington, J.; Glasser, N.F.; Hambrey, M.J.; Reynolds, J.M. Structure-from-Motion' photogrammetry: A low-cost, effective tool for geoscience applications. *Geomorphology* **2012**, *179*, 300–314. [CrossRef]
62. Remondino, F.; El-hakim, S. Image-based 3D modelling: A review. *Photogramm. Rec.* **2006**, *21*, 269–291. [CrossRef]
63. Colomina, I.; Molina, P. Unmanned aerial systems for photogrammetry and remote sensing: A review. *ISPRS J. Photogramm. Remote Sens.* **2014**, *92*, 79–97. [CrossRef]
64. Edelman, G.J.; Aalders, M.C. Photogrammetry using visible, infrared, hyperspectral and thermal imaging of crime scenes. *Forensic Sci. Int.* **2018**, *292*, 181–189. [CrossRef] [PubMed]
65. Dabous, S.A.; Al-Ruzouq, R.; Llort, D. Three-dimensional modeling and defect quantification of existing concrete bridges based on photogrammetry and computer aided design. *Ain Shams Eng. J.* **2023**, *14*, 102231. [CrossRef]
66. Wu, J.; Shi, Y.; Wang, H.; Wen, Y.; Du, Y. Surface Defect Detection of Nanjing City Wall Based on UAV Oblique Photogrammetry and TLS. *Remote. Sens.* **2023**, *15*, 2089. [CrossRef]

67. Califano, N.; Murakami, D. *3D Localization of Defects in Facility Inspection*; National Aeronautics and Space Administration (NASA): Melbourne, FL, USA, 2020. Available online: https://ntrs.nasa.gov/api/citations/20205000516/downloads/FCRAR2020.pdf (accessed on 30 December 2024).
68. Stathopoulou, E.K.; Welponer, M.; Remondino, F. Open-source image-based 3D reconstruction pipelines: Review, comparison and evaluation. In *International Archives of the Photogrammetry, Remote Sensing and Spatial Information Sciences—ISPRS Archives*; Copernicus GmbH for the International Society for Photogrammetry and Remote Sensing (ISPRS): Göttingen, Germany, 2019; pp. 331–338. [CrossRef]
69. Lowe, D.G. Distinctive Image Features from Scale-Invariant Keypoints. November 2004. Available online: https://link.springer.com/article/10.1023/B:VISI.0000029664.99615.94 (accessed on 30 December 2024).
70. Alcantarilla, P.F.; Nuevo, J.; Bartoli, A. Fast Explicit Diffusion for Accelerated Features in Nonlinear Scale Spaces. In Proceedings of the BMVC 2013—Electronic Proceedings of the British Machine Vision Conference, Bristol, UK, 9–13 September 2013; British Machine Vision Association, BMVA. pp. 1281–1298. Available online: https://bmva-archive.org.uk/bmvc/2013/Papers/paper0013/abstract0013.pdf (accessed on 18 March 2025). [CrossRef]
71. Schönberger, J.L.; Price, T.; Sattler, T.; Frahm, J.-M.; Pollefeys, M. A Vote-and-Verify Strategy for Fast Spatial Verification in Image Retrieval. In Proceedings of the Computer Vision–ACCV 2016: 13th Asian Conference on Computer Vision, Taipei, Taiwan, 20–24 November 2016. [CrossRef]
72. Schönberger, J.L.; Frahm, J.-M. Structure-from-Motion Revisited. In Proceedings of the IEEE Conference on Computer Vision and Pattern Recognition, Las Vegas, NV, USA, 27–30 June 2016. [CrossRef]
73. Muja, M.; Lowe, D.G. Fast Approximate Nearest Neighbors with Automatic Algorithm Configuration. In Proceedings of the International Conference on Computer Vision Theory and Applications, Lisbon, Portugal, 5–8 February 2009. Available online: https://www.cs.ubc.ca/~lowe/papers/09muja.pdf (accessed on 30 December 2024).
74. Cheng, J.; Leng, C.; Wu, J.; Cui, H.; Lu, H. Fast and Accurate Image Matching with Cascade Hashing for 3D Reconstruction. In Proceedings of the 2014 IEEE Conference on Computer Vision and Pattern Recognition (CVPR), Columbus, OH, USA, 23–28 June 2014. Available online: https://openaccess.thecvf.com/content_cvpr_2014/papers/Cheng_Fast_and_Accurate_2014_CVPR_paper.pdf (accessed on 30 December 2024).
75. Hartley, R.; Zisserman, A. *Multiple View Geometry in Computer Vision*, 2nd ed.; Cambridge University Press: Cambridge, UK, 2003. [CrossRef]
76. Stewénius, H.; Engels, C.; Nistér, D. Recent developments on direct relative orientation. *J. Photogramm. Remote Sens.* **2006**, *60*, 284–294. [CrossRef]
77. Srajer, F. Image Matching for Dynamic Scenes. May 2016. Available online: https://dspace.cvut.cz/bitstream/handle/10467/64771/MU-DP-2016-posudek-Sara_Radim.pdf (accessed on 30 December 2024).
78. Gao, X.-S.; Hou, X.-R.; Tang, J.; Cheng, H.-F. Complete Solution Classification for the Perspective-Three-Point Problem. *IEEE Trans. Pattern Anal. Mach. Intell.* **2003**, *25*, 930–943. [CrossRef]
79. Lepetit, V.; Moreno-Noguer, F.; Fua, P. EPnP: An Accurate O(n) Solution to the PnP Problem. *Int. J. Comput. Vis.* **2008**, *81*, 155–166. [CrossRef]
80. Agarwal, S.; Mierle, K.; The Ceres Solver Team. Ceres Solver. October 2023. Available online: https://github.com/ceres-solver/ceres-solver (accessed on 16 October 2024).
81. Schönberger, J.L.; Zheng, E.; Pollefeys, M.; Frahm, J.-M. Pixelwise View Selection for Unstructured Multi-View Stereo. In Proceedings of the Computer Vision–ECCV 2016: 14th European Conference, Amsterdam, The Netherlands, 11–14 October 2016. [CrossRef]
82. Shen, S. Accurate Multiple View 3D Reconstruction Using Patch-Based Stereo for Large-Scale Scenes. *IEEE Trans. Image Process.* **2013**, *22*, 1901–1914. [CrossRef]
83. Hirschmüller, H. Stereo Processing by Semiglobal Matching and Mutual Information. *IEEE Trans. Pattern Anal. Mach. Intell.* **2008**, *30*, 328–341. [CrossRef]
84. Alexakis, E.; Delegou, E.T.; Mavrepis, P.; Rifios, A.; Kyriazis, D.; Moropoulou, A. A novel application of deep learning approach over IRT images for the automated detection of rising damp on historical masonries. *Case Stud. Constr. Mater.* **2024**, *20*, e02889. [CrossRef]
85. Wang, C.; Wang, X.; Zhou, X.; Li, Z. The Aircraft Skin Crack Inspection Based on Different-Source Sensors and Support Vector Machines. *J. Nondestruct. Eval.* **2016**, *35*, 46. [CrossRef]
86. Malekzadeh, T.; Abdollahzadeh, M.; Nejati, H.; Cheung, N.-M. Aircraft Fuselage Defect Detection Using Deep Neural Networks. December 2017. Available online: https://arxiv.org/abs/1712.09213 (accessed on 30 December 2024).
87. Krizhevsky, A.; Sutskever, I.; Hinton, G.E. ImageNet Classification with Deep Convolutional Neural Networks. In *Advances in Neural Information Processing Systems*; ISPRS: Lake Tahoe, NV, USA, 2012. Available online: https://papers.nips.cc/paper/2012/file/c399862d3b9d6b76c8436e924a68c45b-Paper.pdf (accessed on 30 December 2024).

88. Chatfield, K.; Simonyan, K.; Vedaldi, A.; Zisserman, A. Return of the Devil in the Details: Delving Deep into Convolutional Nets. In Proceedings of the British Machine Vision Conference (BMVC), Nottinghamshire, UK, 1–5 September 2014; pp. 1–12. Available online: https://arxiv.org/abs/1405.3531 (accessed on 30 December 2024).
89. Bay, H.; Tuytelaars, T.; Van Gool, L. SURF: Speeded Up Robust Features. In Proceedings of the 9th European Conference on Computer Vision (ECCV), Graz, Austria, 7–13 May 2006; Springer: Berlin/Heidelberg, Germany, 2006; pp. 404–417. [CrossRef]
90. Vedaldi, A.; Lenc, K. MatConvNet—Convolutional Neural Networks for MATLAB. May 2016. Available online: https://arxiv.org/abs/1412.4564 (accessed on 31 December 2024).
91. Miranda, J.; Veith, J.; Larnier, S.; Herbulot, A.; Devy, M. Machine learning approaches for defect classification on aircraft fuselage images acquired by a UAV. In Proceedings of the Fourteenth International Conference on Quality Control by Artificial Vision, Mulhouse, France; 2019; pp. 111–124. [CrossRef]
92. Bouarfa, S.; Doğru, A.; Arizar, R.; Aydoğan, R.; Serafico, J. Towards Automated Aircraft Maintenance Inspection. A Use Case of Detecting Aircraft Dents Using Mask R-CNN. In Proceedings of the AIAA Scitech 2020 Forum, Orlando, FL, USA, 6–10 January 2020; American Institute of Aeronautics and Astronautics Inc.: Reston, VA, USA, 2020. [CrossRef]
93. Dutta, A.; Zisserman, A.; Jain, M. The VIA Annotation Software for Images, Audio and Video. Nice, France. October 2019. Available online: https://arxiv.org/abs/1904.10699 (accessed on 31 December 2024).
94. Ren, I.; Zahiri, F.; Sutton, G.; Kurfess, T.; Saldana, C. A Deep Ensemble Classifier for Surface Defect Detection in Aircraft Visual Inspection. *Smart Sustain. Manuf. Syst.* **2020**, *4*, 81–94. [CrossRef]
95. Avdelidis, N.P.; Tsourdos, A.; Lafiosca, P.; Plaster, R.; Plaster, A.; Droznika, M. Defects Recognition Algorithm Development from Visual UAV Inspections. *Sensors* **2022**, *22*, 4682. [CrossRef]
96. Ding, M.; Wu, B.; Xu, J.; Kasule, A.N.; Zuo, H. Visual inspection of aircraft skin: Automated pixel-level defect detection by instance segmentation. *Chin. J. Aeronaut.* **2022**, *35*, 254–264. [CrossRef]
97. Jaeger, B.E.; Schmid, S.; Grosse, C.U.; Gögelein, A.; Elischberger, F. Infrared Thermal Imaging-Based Turbine Blade Crack Classification Using Deep Learning. *J. Nondestr. Eval.* **2022**, *41*, 74. [CrossRef]
98. Oh, X.; Loh, L.; Foong, S.; Koh, Z.B.A.; Ng, K.L.; Tan, P.K.; Toh, P.L.P.; Tan, U.-X. CNN-Based Camera Pose Estimation and Localization of Scan Images for Aircraft Visual InspectionAircraft Visual Inspection. *IEEE Trans. Intell. Transp. Syst.* **2024**, *25*, 8629–8640. [CrossRef]
99. Zhang, X.; Chen, Y.; Hu, J. Recent advances in the development of aerospace materials. *Prog. Aerosp. Sci.* **2018**, *97*, 22–34. [CrossRef]
100. Li, J.; Zhan, D.; Jiang, Z.; Zhang, H.; Yang, Y.; Zhang, Y. Progress on improving strength-toughness of ultra-high strength martensitic steels for aerospace applications: A review. *J. Mater. Res. Technol.* **2023**, *23*, 172–190. [CrossRef]
101. Suomalainen, E.; Celikel, A.; Vénuat, P. Aircraft Metals Recycling: Process, Challenges and Opportunities. 2014. Available online: https://api.semanticscholar.org/CorpusID:214587198 (accessed on 31 December 2024).
102. Tah, B. Manufacturing and Structural Analysis of a Lightweight Sandwich Composite UAV Wing. 2007. Available online: https://etd.lib.metu.edu.tr/upload/12608774/index.pdf (accessed on 31 December 2024).
103. Wong, K.; Rudd, C.; Pickering, S.; Liu, X.L. Composites recycling solutions for the aviation industry. *Sci. China Technol. Sci.* **2017**, *60*, 1291–1300. [CrossRef]
104. Skoczylas, J.; Samborski, S.; Kłonica, M. The Application of Composite Materials in the Aerospace Industry. *J. Technol. Exploit. Mech. Eng.* **2019**, *5*, 1–6. [CrossRef]
105. Sause, M.G.R.; Jasiūnienė, E. *Structural Health Monitoring Damage Detection Systems for Aerospace*; Springer: Berlin/Heidelberg, Germany, 2021. Available online: https://link.springer.com/book/10.1007/978-3-030-72192-3 (accessed on 31 December 2024).
106. Griwodz, C.; Gasparini, S.; Calvet, L.; Gurdjos, P.; Castan, F.; Maujean, B.; De Lillo, G.; Lanthony, Y. AliceVision Meshroom: An open-source 3D reconstruction pipeline. In Proceedings of the MMSys '21: Proceedings of the 12th ACM Multimedia Systems Conference, Istanbul, Turkey, 7–11 September 2021; ACM: New York, NY, USA, 2021; pp. 241–247. [CrossRef]

Advanced diagnostics of aircraft structures using automated non-invasive imaging techniques: a comprehensive review

Bardis, Kostas

2025-04-01

Bardis K, Avdelidis NP, Ibarra-Castanedo C, et al., (2025) Advanced diagnostics of aircraft structures using automated non-invasive imaging techniques: a comprehensive review. Applied Sciences, Volume 15, Issue 7, April 2025, Article number 3584

https://doi.org/10.3390/app15073584